ANNALS OF CARNEGIE MUSEUM

VOL. 87, NUMBER 1, PP. 1–35 15 MAY 2021

THE ELEMENT OF PAAW IN MARSUPIALS AND THE EAR REGION OF *PHILANDER OPOSSUM* (LINNAEUS, 1758) (DIDELPHIMORPHIA, DIDELPHIDAE)

JOHN R. WIBLE
Curator, Section of Mammals, Carnegie Museum of Natural History
5800 Baum Boulevard, Pittsburgh, Pennsylvania 15206
wiblej@carnegiemnh.org

SARAH L. SHELLEY
[Research Associate, Section of Mammals, Carnegie Museum of Natural History]
School of Geosciences, University of Edinburgh, Grant Institute, James Hutton Road, Edinburgh, EH9 3FE, United Kingdom
Sarah.Shelley@ed.ac.uk

CARLY BELZ
Departments of English and Anthropology, University of Pittsburgh
4200 Fifth Ave, Pittsburgh, Pennsylvania 15260
cmb272@pitt.edu

ABSTRACT

A small piece of cartilage or bone, the element of Paaw, occurs in the tendon of the stapedius muscle in some extant marsupial and placental mammals. It has been nearly a century since the last comprehensive treatment of the distribution of the element of Paaw in mammals. The current report updates knowledge on this structure by synthesizing the subsequent literature and providing new observations of extant marsupials from the collections of the Section of Mammals, Carnegie Museum of Natural History, and two online resources for CT scanned data: DigiMorph.org and MorphoSource.org. We found an element of Paaw in some representatives of all seven extant marsupial orders: Didelphimorphia, Microbiotheria, Notoryctemorphia, Peramelemorphia, Paucituberculata, Dasyuromorphia, and Diprotodontia. In the first four orders, the element is substantial, longer than the long axis of the fenestra vestiuli (oval window), which holds the stapedial footplate; it is smaller than the long axis of the fenestra vestibuli in Paucituberculata and we do not have measures to report for the last two orders. In most marsupials examined, the element of Paaw contacts the petrosal behind the oval window, suggesting it functions as a sesamoid bone, increasing the lever arm of the stapedius muscle. Although there is some variability in the presence of the bone both between and within individual museum specimens, we interpret this as the result of preparation techniques rather than true variation.

To place the element of Paaw in its anatomical context, we describe in detail the ear region and middle-ear auditory apparatus of the gray four-eyed opossum, *Philander opossum* (Linnaeus, 1758), a didelphid from Central and South America, based on a CT scanned specimen from Carnegie Museum of Natural History. It has an ossified element of Paaw with a volume greater than the stapes. Comparisons are made with petrosals of *Didelphis marsupialis* Linnaeus, 1758, and *Monodelphis domestica* (Wagner, 1842), also based on CT scanned specimens.

KEY WORDS: didelphids, ectotympanic, element of Paaw, incus, malleus, petrosal, *Philander opossum*, stapes, stapedial ratio

INTRODUCTION

Among extant vertebrates, it is well known that mammals are distinguished by the presence of three small bones in the middle ear, the malleus, incus, and stapes, comprising the ossicular auditus or auditory ossicles, which transmit vibrations from the tympanic membrane to the inner ear. It is less well known that historically two additional bones have been proposed as the os quartum or fourth auditory ossicle: the os lenticulare and the element of Paaw. The os lenticulare or os orbiculare is a small oval or lens-shaped element located between the long process (crus longum) of the incus and the head of the stapes, which was considered by some anatomists even into the latter half of the nineteenth century to be independent of the incus (Asherson 1978; Graboyes et al. 2011b); the currently accepted view is that the os lenticulare is part of the incus (Burford and Mason 2016; Rodríguez-Vázquez et al. 2018) to which it is connected by the processus lenticulare (Nomina Anatomica Veterinaria 2017). The other candidate for the fourth ossicle is the element of Paaw (Graboyes et al. 2011a), a bone occurring in the tendon of the stapedius muscle in some therian mammals (Klaauw 1923; Abdala et al. 2019).

The element of Paaw was first reported in 1615 as a small bone within the tendon of the stapedius muscle in oxen by Pieter Paaw, an anatomist in Leiden (Graboyes et al. 2011a). After this first observation, the element came to be known as the cartilage of Paaw (misspelled Paauw by some according to Hinchcliffe and Pye 1969: 279), or when ossified the os quartum or skeletal element of Paaw. Some authors (e.g., Meng and Hou 2016) hypothesized the element of Paaw to be a remnant of the interhyal (interhyale), which connects the stapes and Reichert's cartilage, the second pharyngeal arch cartilage, during development and gives rise to the stapedius muscle tendon (Rodríguez-Vázquez 2005; Fig. 1). However, there is skepticism about this homology (e.g., Allin and Hopson 1992), and the element may be a neomorph of some mammals given its late ontogenetic appearance (Shute 1956).

Whether the element of Paaw is a fourth auditory ossicle depends on the definition of an auditory ossicle, and in our search of the literature we found that to be a concept not precisely defined. Anatomical treatises, either on human (e.g., Strandring 2008) or domesticated mammals

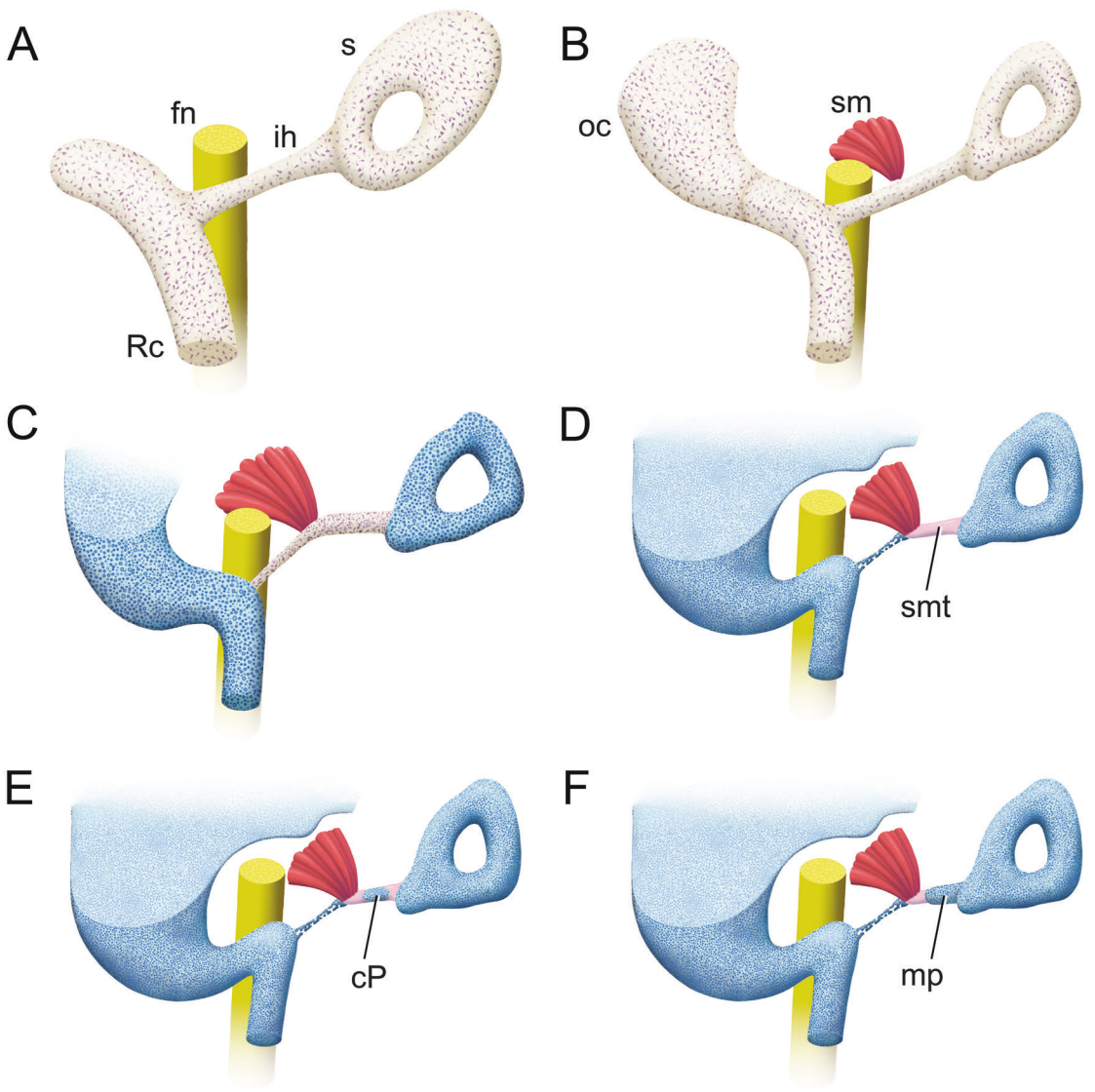

Fig. 1.—Schematic ontogenetic model for the formation of the structures derived from the interhyal; A-D based on Rodríguez-Vázquez (2005); E derived from Shute (1956); F speculative reflecting the condition in some Mesozoic mammals. **A,** mesenchymal stage with Reichert's cartilage connected to the stapes analage by the interhyal; **B,** mesenchymal stage with the stapedius muscle forming; **C,** cartilage (blue) forms in Reichert's cartilage, otic capsule, and stapes; **D, E, F,** three possible outcomes for the segment of the interhyal between the stapedius muscle and stapes (the segment between the stapedius muscle and Reichert's cartilage ultimately disappears in each): **D,** only the tendon of the stapedius muscle forms; **E,** cartilage of Paaw forms in the tendon of the stapedius muscle; **F,** muscular process of the stapes forms; when present in extant mammals, the muscular process is typically subtle (Doran 1878; Henson 1961; Fleischer 1973) but has been found to be quite large in some Mesozoic mammals (Meng and Hou 2016; Meng et al. 2018). Abbreviations: **cP,** cartilage of Paaw; **fn,** facial nerve; **ih,** interhyal; **mp,** muscular process of stapes; **oc,** otic capsule; **Rc,** Reichert's cartilage; **s,** stapes; **sm,** stapedius muscle; **smt,** stapedius muscle tendon.

(e.g., Sisson 1914; Evans 1993), merely describe the malleus, incus, and stapes as auditory ossicles without providing a definition for the term. The same can be said for general treatments of the auditory apparatus (e.g., Henson 1974; Fleischer 1978) and specialized reports on the ossicles themselves (e.g., Doran 1878; Henson 1961; Fleischer 1973). We employ the description by Henson (1961: 159) for the criteria we employ in recognizing auditory ossicles: "The auditory ossicles, *Malleus, incus and stapes,* extend across the tympanic cavity and form a system of levers that morphologically and functionally connects the tympanic membrane with the fluids of the inner ear." Accepting these criteria as a definition, the element of Paaw is not an auditory ossicle as it is not part of the articulated chain but an accessory structure only attached to the stapes by a tendon.

Recently, some fossils of Mesozoic mammals (e.g., the Middle Jurassic haramiyidan *Arboroharamiya allinhopsoni* Han et al., 2017 (Han et al. 2017; Meng et al. 2020) and the Early Cretaceous multituberculate *Sinobaatar pani* Mao et al., 2020 (Mao et al. 2020)) have been reported to have five auditory bones. In addition to the malleus, incus, and stapes, these authors included the ectotympanic, which supports the tympanic membrane, and the surangular, a bone widely present in non-mammalian cynodonts (Allin and Hopson 1992) but of limited and uncertain distribution in Mesozoic mammals (Wang et al. 2021). In explaining their usage, Meng et al. (2020: 52) stated "we use 'auditory bones' to imply the stapes, incus, malleus, ectotympanic, and surangular that are present in *Arboroharamiya allinhopsoni*. We restrict 'middle ear bones' to the first three of the five auditory bones. The auditory bones and the middle ear bones are used interchangeably for the stapes, incus, and malleus." As discussed by Wang et al. (2021), we find this usage unnecessary and confusing. There are many bones of the mammalian basicranium in addition to these five that contribute in myriad ways to the structure of the auditory apparatus (Kampen 1905; Klaauw 1931), including the petrosal, squamosal, alisphenoid, basisphenoid, basioccipital, exoccipital, supraoccipital, entotympanics, and stylohyal. However, in extant mammals, there are only three small bones that form the articulated chain connecting the tympanum and oval window, which are best referred to as auditory or middle ear ossicles.

The last comprehensive review of the distribution of the element of Paaw in therian mammals was by the Leiden zoologist C.J. van der Klaauw in 1923, who reviewed the literature and offered some new observations. We propose to do the same here, to update Klaauw's summary with observations in the literature subsequent to 1923 and also to offer new observations on marsupials. We focus attention on didelphid marsupials, where the element of Paaw is a significant structure, and take the opportunity to describe the ear region of the extant didelphid *Philander opossum* (Linnaeus, 1758) in some detail to put the element of Paaw in context. There is considerable literature on the ear region and auditory apparatus of extant didelphids, both from the standpoint of development (e.g., Toeplitz 1920; Maier 1987; Filan 1991; Clark and Smith 1993; Sánchez-Villagra et al. 2002) and adult morphology (e.g., Segall 1970; Fleischer 1973; Archer 1976; Reig et al. 1987; Wible 1990, 2003; Wible and Hopson 1995; Sánchez-Villagra and Wible 2002; Schmelze et al. 2005). However, *Philander opossum* has not been the subject of intensive study.

MATERIALS AND METHODS

In addition to the literature, there are three primary sources for the specimens investigated here: (1) the research collections of the Section of Mammals, Carnegie Museum of Natural History (CM), Pittsburgh; (2) DigiMorph.org; and (3) MorphoSource.org.

Regarding #1, 470 CM marsupial specimens were studied with a stereomicroscope. One specimen, the didelphid *Philander opossum*, CM 110578, an adult female collected March 18, 1993 in El Salvador, was CT scanned at the Center for Quantitative Imaging, The Pennsylvania State University. The basicranium was scanned with the 300 kV microfocus directional tube of the GE v|tome|x L300 X-ray CT Scanner. The 360° specimen rotation produced 1701 equally spaced images, the exposure time per projection was 500.084 milliseconds, and three frames were averaged for each of the 1700 images. Voltage was 180 kV, current 60 µA, and voxel size 0.012 mm. The elements of the middle ear were segmented manually slice by slice using the pencil segmentation tool and measured in Avizo 2019.4 (Thermo Fischer Scientific, Waltham, Massachusetts).

Regarding #2, Digital Morphology at the University of Texas at Austin (DigiMorph.org) is a repository for digital imagery. Skulls/heads of 36 extant marsupial specimens (Appendix 1), four extant monotremes, and 169 extant placentals had coronal slice movies that we could access as of April 6, 2021. We studied these movies slice by slice in the area of interest.

Regarding #3, MorphoSource by Duke University (MorphoSource.org) is a repository for digital imagery. Stacks of Tiff files resulting from CT scans were downloaded for nine marsupials (Appendix 1); the choice of taxa was constrained by our ability to access them during the time frame of the project. Measurements were made in Avizo 2019.4.

The anatomical terminology employed here follows prior studies by the senior author (e.g., Wible 2003, 2009, 2010) with terms for the auditory ossicles following Henson (1961). Unless noted, soft tissue structures are interpreted for *Philander opossum*, CM 110578, based on the senior author's prior study of *Monodelphis* Burnett, 1830 (Wible 2003, personal observations). Taxonomic usage follows Wilson and Reeder (2005).

Institutional Abbreviations

AMNH—Department of Mammalogy, American Museum of Natural History, New York, New York, USA.

CM—Section of Mammals, Carnegie Museum of Natural History, Pittsburgh, Pennsylvania, USA.

DU BAA—Department of Biological Anthropology and Anatomy, Duke University, Durham, North Carolina, USA.

DU EA—Department of Evolutionary Anthropology, Duke University, Durham, North Carolina, USA.

FMNH—Field Museum of Natural History, Chicago, Illinois, USA.

KU—Division of Mammalogy, Biodiversity Institute and Natural History Museum, The University of Kansas, Lawrence, Kansas, USA.

NMV—Museum Victoria, Melbourne, Australia.

TTM—Texas Memorial Museum, The University of Texas at Austin, Austin, Texas, USA.
UMMZ—Division of Mammals, Museum of Zoology, University of Michigan, Ann Arbor, Michigan, USA.
UMZC—Museum of Zoology, University of Cambridge, Cambridge, United Kingdom.
USNM—National Museum of Natural History, Smithsonian Institution, Washington, D.C., USA.

RESULTS

Ear Region of *Philander opossum*, CM 110578

Overview.—The central bone of the ear region is the petrosal, which houses the inner ear and supports structures of the middle ear. In ventral view (Fig. 2), the petrosal has extensive sutural contacts with the basioccipital and exoccipital medially, the alisphenoid anteriorly, the squamosal laterally, and the exoccipital posteriorly. CM 115078 does not preserve a suture between the basi- and exoccipital, but based on juveniles (e.g., CM 76735), the suture is situated just anterior to the foramen for the inferior petrosal sinus ("fips" in Fig. 2). The petrosal also has a point contact with the basisphenoid anteromedially at the posteromedial corner of the foramen for the greater petrosal nerve ("fgpn" in Fig. 2); there is no suture between the basi- and alisphenoid but we follow the usual convention of delimiting the basisphenoid on the central stem and the alisphenoid as the wing. There are only three foramina bordered by the petrosal in ventral view. Posteromedially, between the exoccipital and petrosal is the jugular foramen ("jf" in Fig. 2), which following the models of *Didelphis virginiana* Kerr, 1792, and *Monodelphis domestica* (Wagner, 1842) (Wible 2003) transmits cranial nerves IX, X, and XI and no significant vein; the major exit for the sigmoid sinus is via a venous sulcus ("vs" in Fig. 3) directed at the foramen magnum. At the anterior pole of the petrosal are two small openings bordered by the alisphenoid: the piriform fenestra laterally and the foramen for the greater petrosal nerve medially ("pf" and "fgpn," in Fig. 2, respectively), as reported in *Monodelphis domestica* (Wible 2003); the foramen for the greater petrosal nerve also has a small contribution from the basisphenoid. Another opening subequal in size and anteromedial to the jugular foramen is entirely within the exoccipital but close to the petrosal, the foramen for the inferior petrosal sinus. A crest extends posteromedially from the medial aspect of this foramen to the posterior of the two hypoglossal foramina ("hf" in Fig. 2). On the specimen's right side, the foramen for the inferior petrosal sinus is between the exoccipital and petrosal.

In oblique posterolateral view (Fig. 4), the petrosal is largely hidden from view by the overlying squamosal and the elements of the auditory apparatus. The exposure of the petrosal on the occiput is a narrow sliver between the squamosal laterally and the exoccipital medially, with the supraoccipital capping the petrosal dorsally.

The middle ear is situated lateral and anterolateral to the petrosal. A complete bony auditory bulla surrounding the middle ear is lacking. However, processes from the petrosal and its neighbors contribute to a partial bulla with the gaps between these elements presumably completed by connective tissue. The convex tympanic process of the alisphenoid ("tpas" in Fig. 2) is the largest contributor to the partial bulla, covering roughly the anterior half of the middle ear. The intratympanic surface of the alisphenoid tympanic process is smooth and concave, forming a large hypotympanic sinus ("hsas" in Fig. 4) of the middle ear cavity, following the terminology of Klaauw (1931) and Archer (1976). The anterior extratympanic aspect of the alisphenoid tympanic process forms the posterior border of the foramen ovale ("fo" in Fig. 2), the exit for the mandibular division of the trigeminal nerve, cranial nerve V. Along the lateral aspect of the alisphenoid tympanic process are several openings, which vary in number and degree of closure between the right and left sides. On the left side, there are two incisures and three foramina, whereas on the right there are four incisures and five foramina. The anteriormost incisure on both sides is interpreted as the Glaserian fissure ("Gf" in Fig. 2) for the chorda tympani nerve, based on the position of the part of the malleus transmitting that structure (see below). The role of the other openings is unknown. In the juvenile CM 76745, only the opening interpreted as the Glaserian fissure is present.

The squamosal and exoccipital make minor contributions to the partial bulla. The small contribution from the squamosal is the posttympanic crest ("ptcr" in Figs. 2, 4), which is directed ventromedially. In posterolateral view, the arch on the squamosal between the postglenoid process anteriorly ("pgp" in Fig. 4) and the posttympanic crest posteriorly represents the dorsal margin of the bony external acoustic meatus. Regarding the exoccipital, there is a sliver of bone that extends anteriorly from the base of the paracondylar process ("pcp" in Fig. 2) on the left side only. This bone appears to be continuous with the exoccipital and we tentatively identify it as an exoccipital tympanic process ("tpeo" in Figs. 2, 4). There is a small, dorsoventrally oriented foramen of unknown function in the base of this tympanic process. We did not find any comparable structure in the CM *Philander opossum* sample except in CM 76748, which had a very small, isolated bony nodule abutting the caudal tympanic process of the petrosal (see below) in a similar location on the right side. The function of these structures is uncertain.

For completeness, we illustrate the endocranial aspect of the petrosal as this surface is often overlooked (Fig. 3). The anterior border of the petrosal contacts the alisphenoid, with a narrow contact dorsally with the squamosal; ventrally the piriform fenestra and foramen for the greater petrosal nerve are visible in the alisphenoid-petrosal contact. The squamosal has two small exposures: one in the rear of the middle cranial fossa ("mcf" in Fig. 3) where the alisphenoid and parietal are the major contributors and the other along the anterodorsal border of the petrosal. Posterior to its contact with the squamosal, the dorsal border of

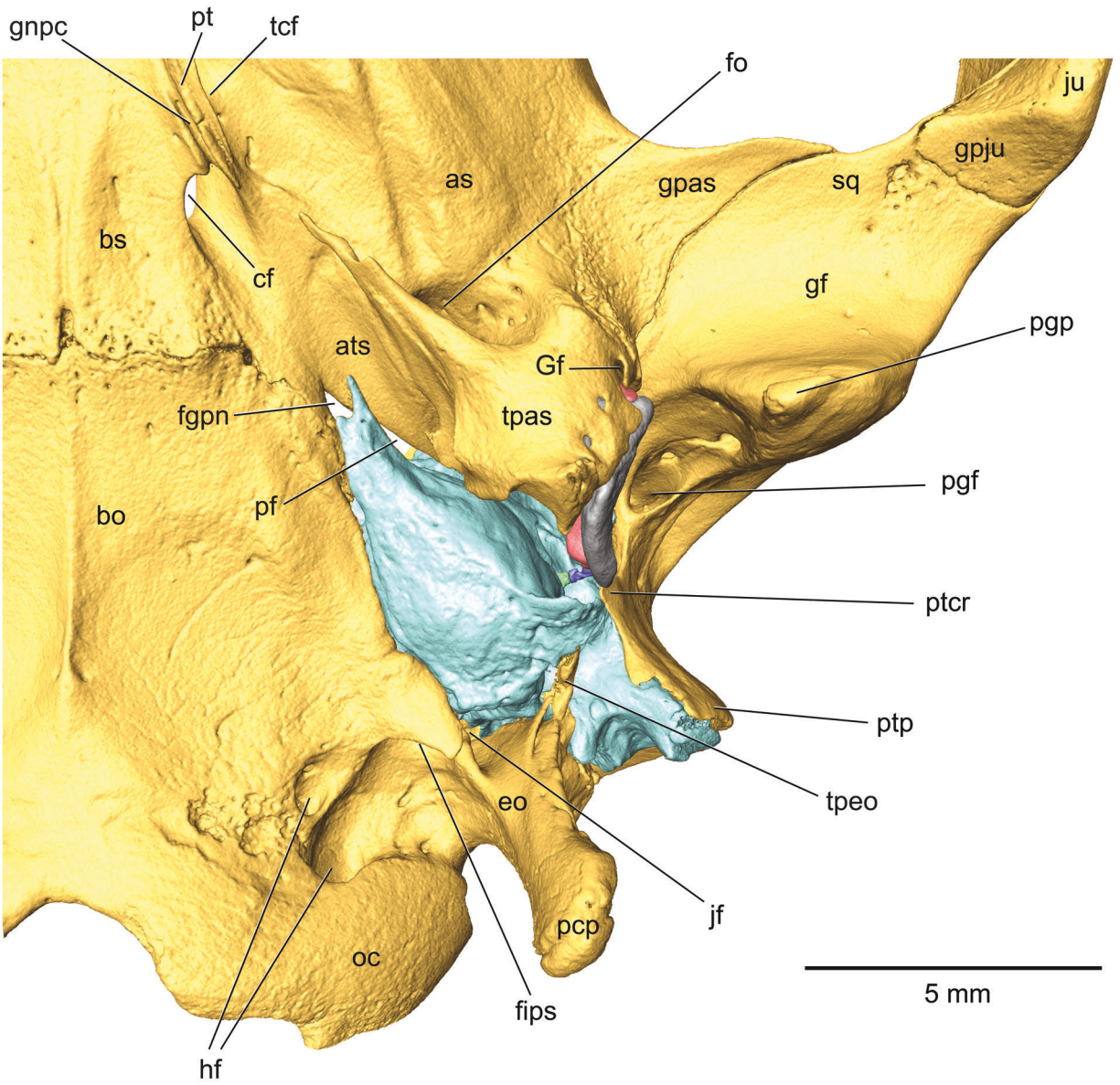

Fig. 2.—Isosurface rendered from CT data of left basicranium of *Philander opossum*, CM 110578, in ventral view; anterior to the top of the page. Petrosal = light blue; ectotympanic = gray; malleus = red; incus = dark blue; stapes = green (barely visible medial to incus). Abbreviations: **as,** alisphenoid; **ats,** auditory tube sulcus; **bo,** basioccipital; **bs,** basisphenoid; **cf,** carotid foramen; **eo,** exoccipital; **fgpn,** foramen for greater petrosal nerve; **fips,** foramen for inferior petrosal sinus; **fo,** foramen ovale; **gf,** glenoid fossa; **Gf,** Glaserian fissure; **gnpc,** groove for nerve of pterygoid canal; **gpas,** glenoid process of alisphenoid; **gpju,** glenoid process of jugal; **hf,** hypoglossal foramen; **jf,** jugular foramen; **ju,** jugal; **oc,** occipital condyle; **pcp,** paracondylar process; **pf,** piriform fenestra; **pgf,** postglenoid foramen; **pgp,** postglenoid process; **pt,** pterygoid; **ptcr,** posttympanic crest; **ptp,** posttympanic process; **sq,** squamosal; **tcf,** transverse canal foramen; **tpas,** tympanic process of alisphenoid; **tpeo,** tympanic process of exoccipital.

the petrosal contacts the parietal anteriorly and the interparietal posteriorly; the parietal and squamosal house a large sulcus for the transverse sinus ("ts" in Fig. 3). The posterior border of the petrosal contacts the exoccipital exclusively. The exoccipital houses the broad venous sulcus transmitting the sigmoid sinus out of the foramen magnum and borders the jugular foramen. Ventrally, the petrosal contacts the basisphenoid anteriorly and the basioccipital behind that. Both of these bones contribute to the large sulcus transmitting the inferior petrosal sinus ("sips" in Fig. 3). The sutural area between the basisphenoid and basioccipital across the midline is essentially flat, that is, a raised dorsum sellae posterior to the hypophyseal fossa ("hyf" in Fig. 3) is lacking.

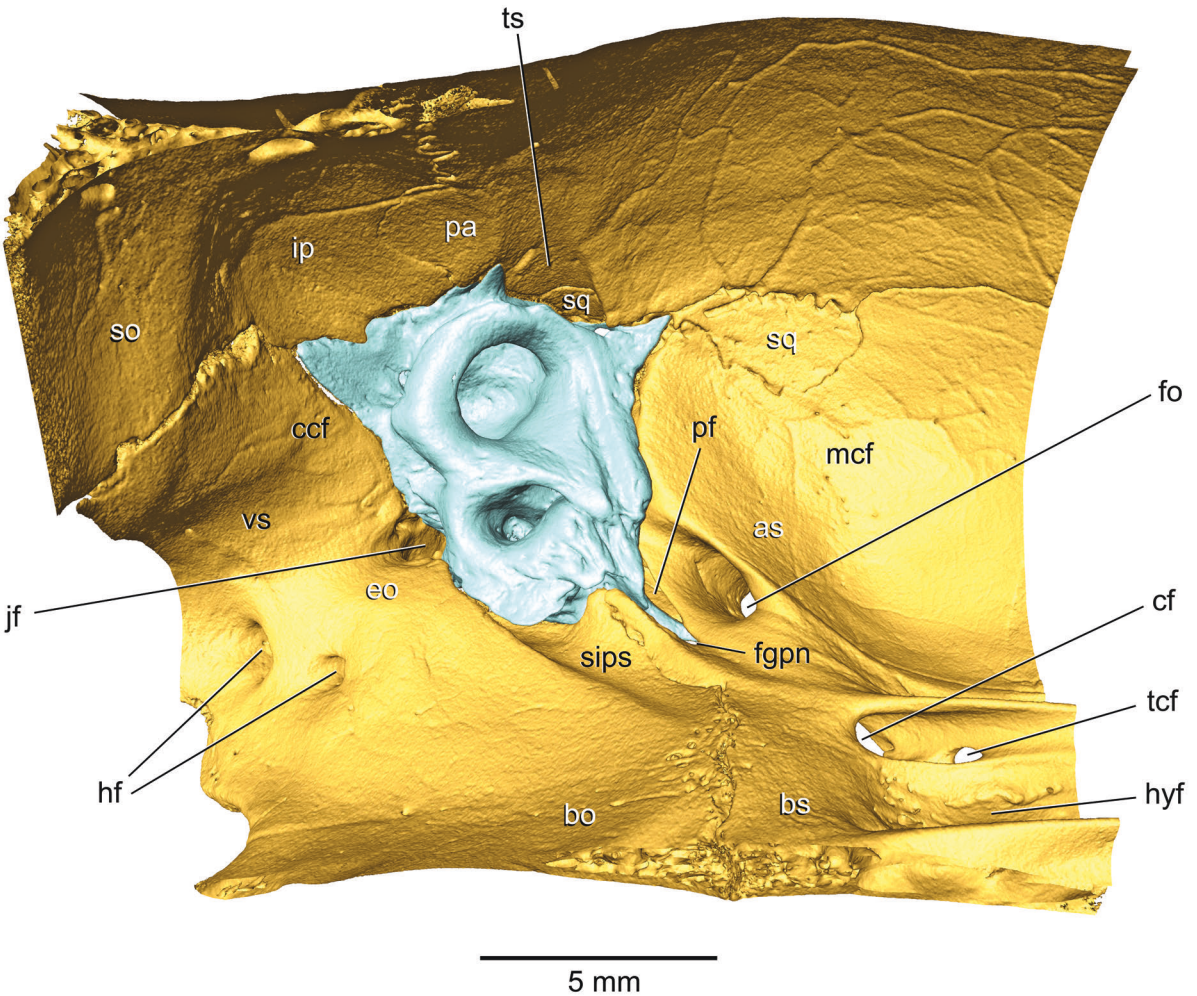

Fig. 3.—Isosurface rendered from CT data of left basicranium of *Philander opossum*, CM 110578, in dorsomedial view; anterior to the right. Petrosal = light blue. Abbreviations: **as,** alisphenoid; **bo,** basioccipital; **bs,** basisphenoid; **ccf,** caudal cranial fossa; **cf,** carotid foramen; **eo,** exoccipital; **fo,** foramen ovale; **fgpn,** foramen for greater petrosal nerve; **hf,** hypoglossal foramen; **hyf,** hypophyseal fossa; **ip,** interparietal; **jf,** jugular foramen; **mcf,** middle cranial fossa; **pf,** piriform fenestra; **sips,** sulcus for inferior petrosal sinus; **so,** supraoccipital; **sq,** squamosal; **tcf,** transverse canal foramen; **ts,** transverse sinus; **vs,** venous sulcus.

Petrosal.—The petrosal is composed of two parts, the pars cochlearis enclosing the cochlea and utricle and the pars canalicularis enclosing the saccule and semicircular canals. There is not a distinct boundary between these two parts: in ventral view (Fig. 5a), the pars cochlearis includes the promontorium and bone anteromedial to it and the pars canalicularis includes the bone lateral and posterior to the promontorium.

The promontorium ("pr" in Fig. 5) is circular in ventral view enclosing the coils of the cochlea ("co" in Figs. 5C–D), which following the method of Ekdale (2013) encompass 900° or 2.5 coils. From the promontorium, the pars cochlearis tapers anteriorly to a point that contacts the alisphenoid, separating the piriform fenestra laterally from the foramen for the greater petrosal nerve medially. Running on the ventral surface of this tapered part of the pars cochlearis is a faint ridge, which represents the base of an anterior septum ("asp" in Fig. 5A). Extending from the anterolateral aspect of the promontorium is a narrow horizontal shelf, the epitympanic wing ("ew" in Fig. 5A). A shallow tensor tympani fossa occupies the medial aspect of the epitymmpanic wing ("ttf" in Fig. 5A), but is largely hidden in ventral view. The promontorium is devoid of any vascular or nervous grooves. At the posteromedial aspect of the promontorium is a triangular process that extends ventrally and then ventrolaterally, the rostral tympanic process ("rtp" in Fig. 5A), which contributes to the partial bulla. At the posterior and posterolateral aspects of the promontorium are two oval openings of similar size and dimensions, the fenestra cochleae (round window) and fenestra vestibuli (oval window), respectively ("fc" and "fv" in Fig. 5C). The latter has a ratio (length to width) of 1.60.

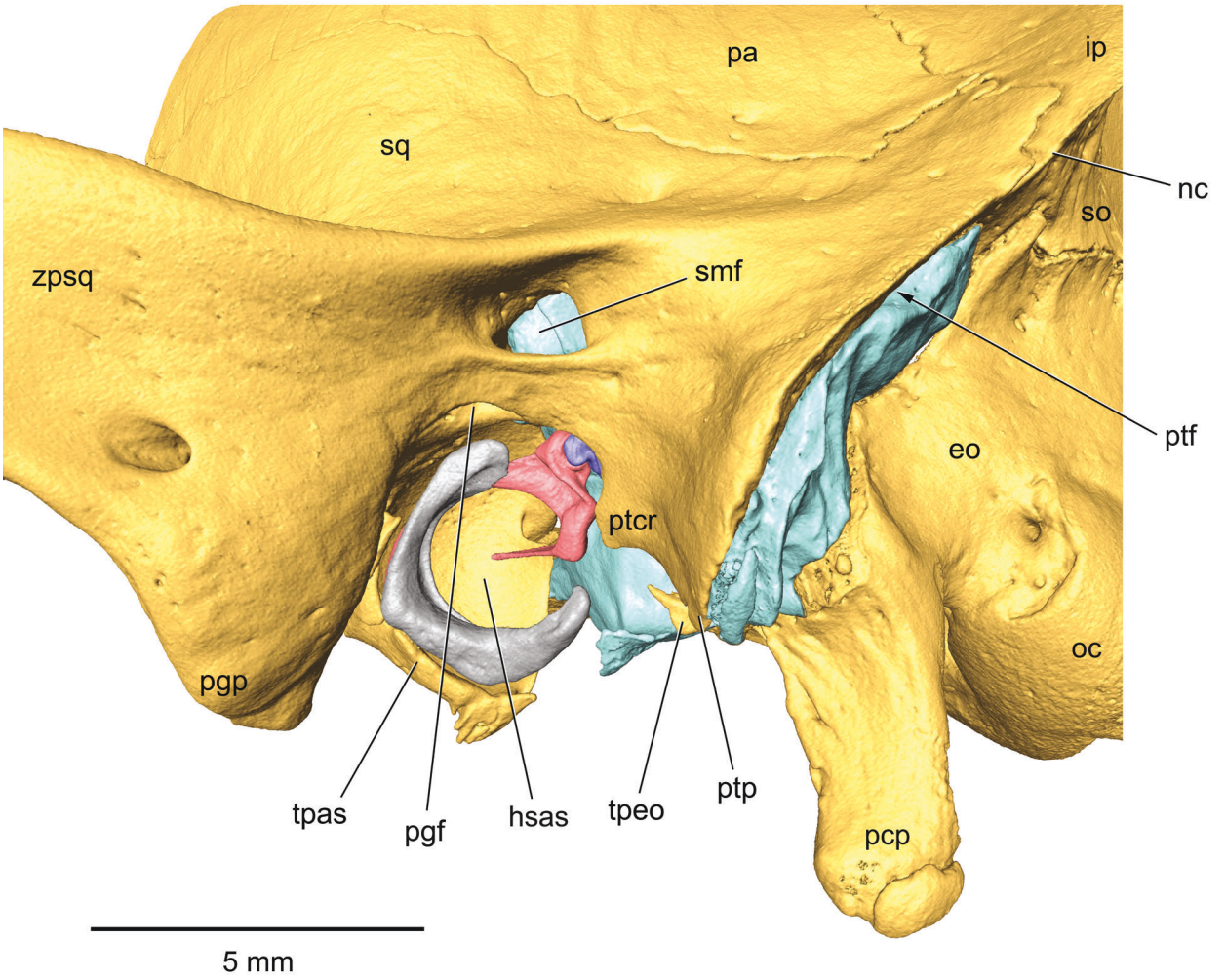

Fig. 4.—Isosurface rendered from CT data of left basicranium of *Philander opossum*, CM 110578, in posterolateral view; anterior to the left. Petrosal = light blue; ectotympanic = gray; malleus = red; incus = dark blue. Abbreviations: **eo,** exoccipital; **hsas,** hypotympanic sinus of alisphenoid; **ip,** interparietal; **nc,** nuchal crest; **oc,** occipital condyle; **pa,** parietal; **pcp,** paracondylar process; **pgf,** postglenoid foramen; **pgp,** postglenoid process; **ptcr,** posttympanic crest; **ptf,** posttemporal foramen; **ptp,** posttympanic process; **smf,** suprameatal foramen; **so,** supraoccipital; **sq,** squamosal; **tpas,** tympanic process of alisphenoid; **tpeo,** tympanic process of exoccipital; **zpsq,** zygomatic process of squamosal.

The round window is not recessed in from the promontorial surface and a cochlear fossula is absent; the posterior half of the oval window is slightly recessed forming a shallow vestibular fossula. Separating the two windows is a thick crista interfenestralis ("ci" in Fig. 5A) that is broader than the long dimension of either window. The crista is not flat but has a significant bulge along is dorsolateral aspect, extending between the oval and round windows. Dorsal to this bulge is a faint sulcus directed at the oval window.

Lateral and posterior to the promontorium are triangular shelves comprising the pars canalicularis, the former smaller and in a more dorsal plane than the latter (Fig. 5A). The lateral shelf is widest anteriorly where its lateral margin has a ventrally-directed crest. Medial to this crest is a concave surface, the epitympanic recess ("er" in Fig. 5A), forming the roof over the incudomallear articulation (Fig. 5B; Klaauw 1931). The area of this ventrally-directed crest represents the tegmen tympani ("tt" in Fig. 5A) (see discussion on the tegmen tympani in Sánchez-Villagra and Forasiepi 2017), the dorsoventral extent of which is seen in lateral view (Fig. 6A). Between the epitympanic recess and promontorium is the broad facial sulcus ("fs" in Fig. 5A) at the anterior end of which is the secondary facial foramen ("sff" in Fig. 5A), both transmitting the facial nerve, cranial nerve VII. At the anteromedial corner of the lateral shelf is the large hiatus Fallopii ("hF" in Fig. 5A) for the greater petrosal nerve, a branch of the facial nerve. The bone between the hiatus Fallopii and secondary facial foramen represents the floor of the cavum supracochleare, the space within the petrosal housing the geniculate ganglion of the facial nerve. Following the characterization of the hiatus position in Sánchez-Villagra and Wible (2002), CM 110578 has an intermediate hiatus Fallopii, with the roof and floor of the

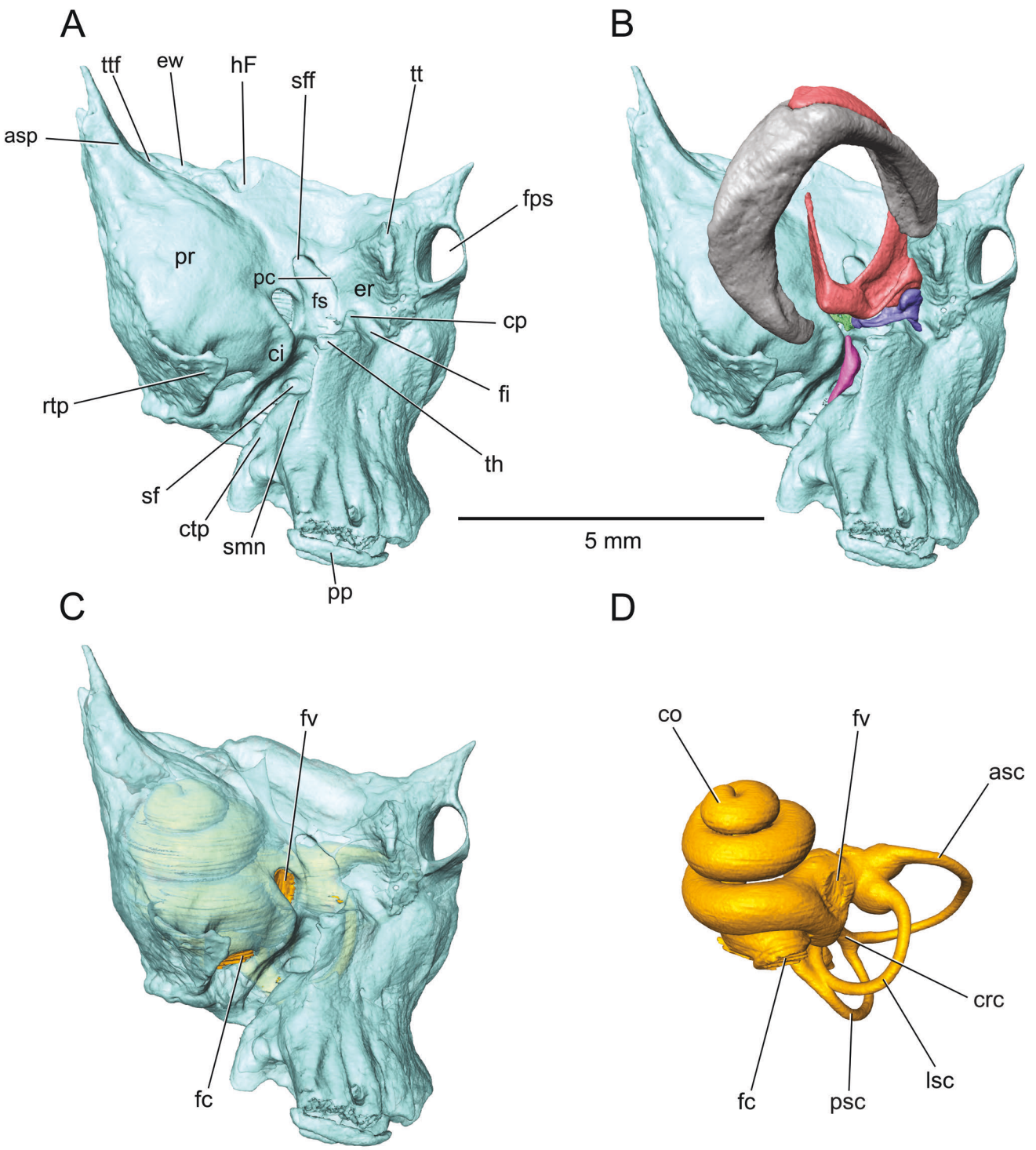

Fig. 5.—Isosurfaces rendered from CT data of left auditory elements of *Philander opossum*, CM 110578, in oblique ventral view; anterior to the top of the page. **A,** petrosal; **B,** petrosal, ectotympanic (gray), malleus (red), incus (dark blue), stapes (green) (barely visible medial to incus), and element of Paaw (purple); **C,** transparent petrosal with inner ear; **D,** inner ear. Abbreviations: **asc,** anterior semicircular canal; **asp,** anterior septum; **ci,** crista interfenestralis; **co,** cochlea; **cp,** crista parotica; **crc,** crus commune; **ctp,** caudal tympanic process; **end,** endolymphatic duct; **ew,** epitympanic wing; **fc,** fenestra cochleae; **fi,** fossa incudis; **fps,** foramen for prootic sinus; **fs,** facial sulcus; **fv,** fenestra vestibuli; **hF,** hiatus Fallopii; **lsc,** lateral semicircular canal; **pc,** prootic canal; **pp,** paroccipital process; **pr,** promontorium; **psc,** posterior semicircular canal; **rtp,** rostral tympanic process; **sf,** stapedius fossa; **sff,** secondary facial foramen; **smn,** stylomastoid notch; **sps,** sulcus for prootic sinus; **th,** tympanohyal; **tt,** tegmen tympani; **ttf,** tensor tympani fossa.

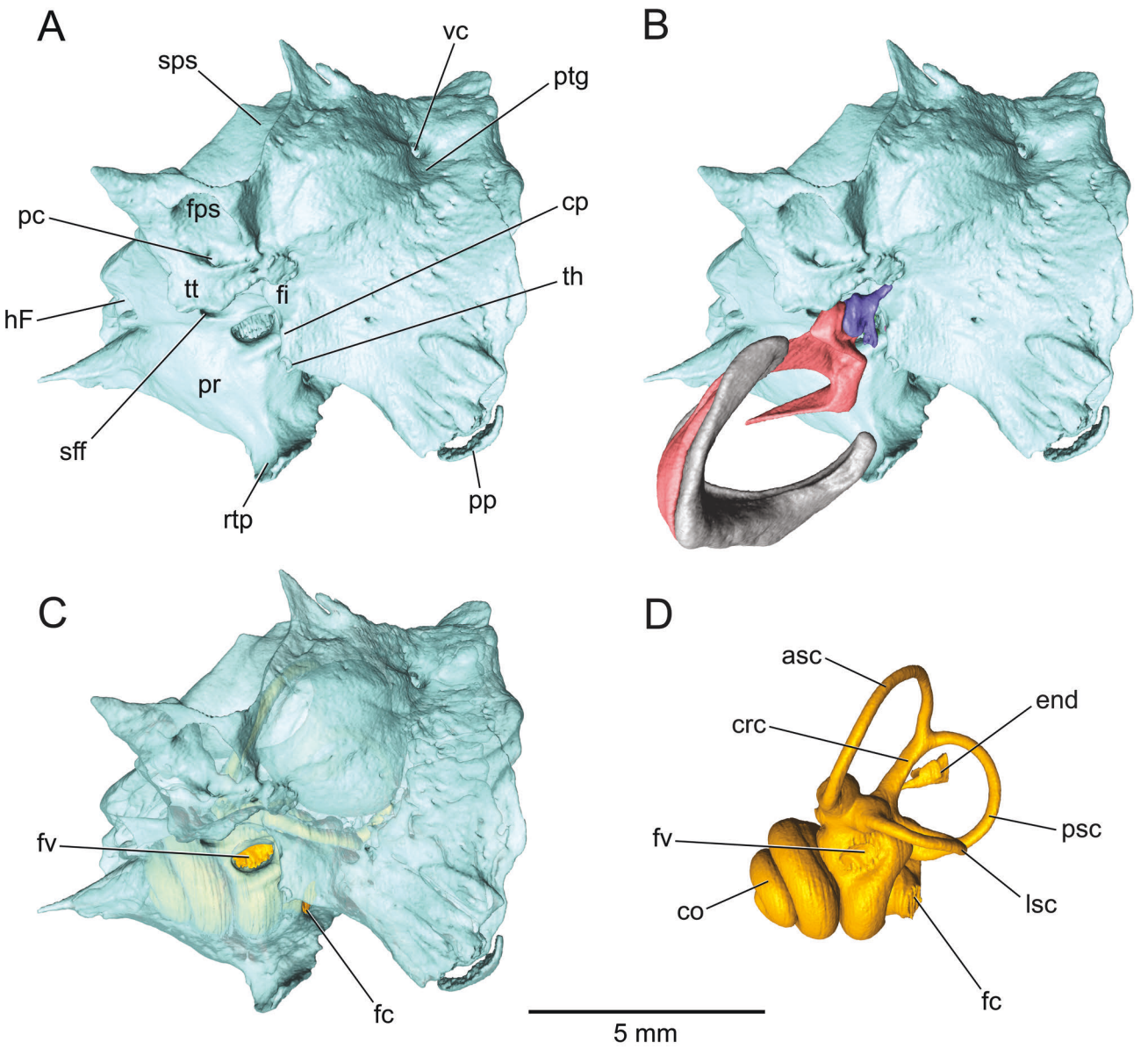

Fig. 6.—Isosurfaces rendered from CT data of left auditory elements of *Philander opossum*, CM 110578, in posterolateral view; anterior to the left. **A,** petrosal; **B,** petrosal, ectotympanic (gray), malleus (red), and incus (dark blue); **C,** transparent petrosal with inner ear; **D,** inner ear. Abbreviations: **asc,** anterior semicircular canal; **co,** cochlea; **cp,** crista parotica; **crc,** crus commune; **fc,** fenestra cochleae; **fi,** fossa incudis; **fps,** foramen for prootic sinus; **fv,** fenestra vestibuli; **hF,** hiatus Fallopii; **lsc,** lateral semicircular canal; **pc,** prootic canal; **pp,** paroccipital process; **pr,** promontorium; **psc,** posterior semicircular canal; **ptg,** posttemporal groove; **rtp,** rostral tympanic process; **sff,** secondary facial foramen; **sps,** sulcus for prootic sinus; **th,** tympanohyal; **tt,** tegmen tympani; **vc,** vascular canal.

cavum supracochleare extending anteriorly to the same extent. Hidden in the anterolateral aspect of the facial sulcus is a small vascular foramen ("pc" in Fig. 5A) leading into a canal that runs dorsal to the epitympanic recess and opens laterally in the sulcus for the prootic sinus ("sps" in Fig. 6A); this is the prootic canal, which transmits the prootic sinus to the lateral head vein (Rougier and Wible 2006); the former drains from the transverse sinus endocranially and the latter runs posteriorly in the facial sulcus.

The shelf posterior to the promontorium has at its posterior apex the rounded paroccipital process ("pp" in Fig. 5 A), which is covered laterally by the posttympanic process of the squamosal ("ptp" in Figs. 2, 4). The paroccipital process is not fully ossified, as denoted by the gap separating it from the rest of the petrosal (Fig. 6A), which would have been filled with cartilage in life. Ascending anteriorly from the paroccipital process is a crest, most easily visualized in lateral view (Fig. 6A). This crest represents the

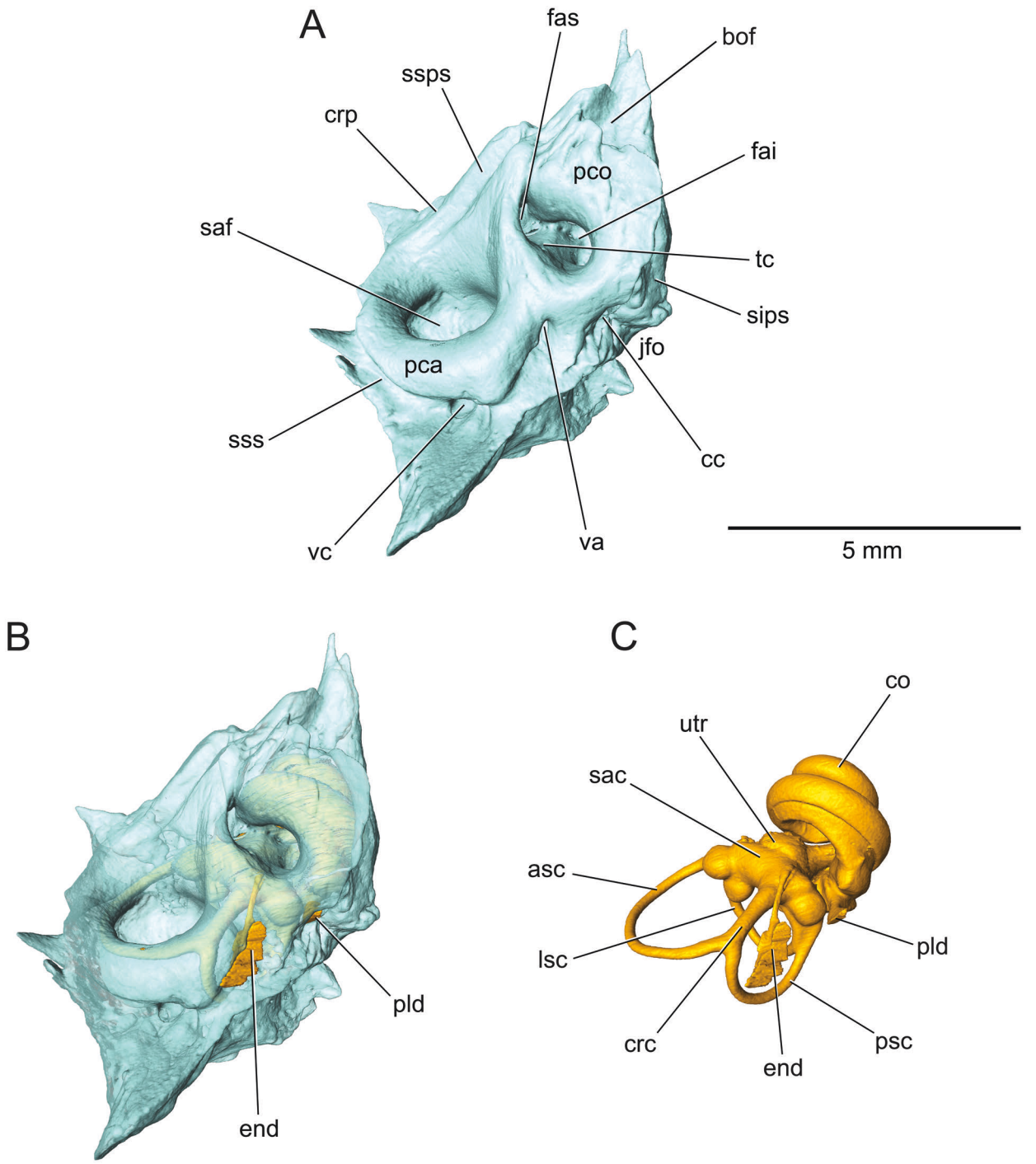

Fig. 7.—Isosurfaces rendered from CT data of left auditory elements of *Philander opossum*, CM 110578, in dorsomedial view; anterior to the top of the page. **A,** petrosal; **B,** transparent petrosal with inner ear; **C,** inner ear. Abbreviations: **asc,** anterior semicircular canal; **bof,** basioccipital facet; **cc,** cochlear canaliculus; **co,** cochlea; **crc,** crus commune; **crp,** crista petrosa; **end,** endolymphatic duct; **fai,** foramen acusticum inferius; **fas,** foramen acusticum superius; **jfo,** jugular fossa; **lsc,** lateral semicircular canal; **pca,** pars canalicularis; **pco,** pars cochlearis; **pld,** perilymphatic duct; **psc,** posterior semicircular canal; **sac,** saccule; **saf,** subarcuate forra; **sips,** sulcus for inferior petrosal sinus; **ssps,** sulcus for superior petrosal sinus; **sss,** sulcus for sigmoid sinus; **tc,** transverse crest; **utr,** utricle; **va,** vestibular aqueduct; **vc,** vascular canal.

crista parotica ("cp" in Fig. 6A), which ends in the rear of the epitympanic recess (Fig. 5A). There is an inflection point on this crest where it turns sharply dorsally; this is the tympanohyal ("th" in Fig. 6A), the point of attachment of Reichert's cartilage. The segment of the crista parotica anterior to the tympanohyal forms the medial wall of the fossa incudis ("fi" in Fig. 6A), housing the crus breve of the incus; the petrosal also forms the roof of the fossa, with the squamosal comprising the lateral wall. The fossa incudis is continuous with and much smaller than the epitympanic recess (Fig. 5A). Posteromedial to the tympanohyal is the exit point of the facial nerve from the middle ear, the stylomastoid notch ("smn" in Fig. 5A). A crest arises from the medial margin of the stylomastoid notch and extends posteromedially, separated from the rear of the promontorium by a gap; this crest is the lateral section of the caudal tympanic process ("ctp" in Fig. 5A; MacPhee 1981; Wible and Shelley 2020). At its medial end, the caudal tympanic process is covered by the exoccipital (Fig. 2). The space between the caudal tympanic process and promontorium is the post-promontorial tympanic sinus (Wible 1990). In the lateral aspect of the sinus is the stapedius fossa ("sf" in Fig. 5A), which houses the stapedius muscle. The stapedius fossa is oval with its long dimension nearly three times that of the oval window. Medial to the sinus is the jugular foramen, which is roughly twice the size of the round window.

Between the exoccipital and squamosal, the posterior surface of the pars canalicularis is exposed on the occiput (Fig. 4), usually referred to as the mastoid exposure. In ventral view (Fig. 2), the ventral margin of the mastoid exposure is U-shaped, which houses a muscular fossa that occupies the ventral third of the mastoid exposure; based on muscle attachment in *Didelphis virginiana* (Coues 1872), this fossa houses the sternomastoid and cleidomastoid. In the dorsolateral margin of the mastoid exposure is the posttemporal foramen, which is completed laterally by the squamosal ("ptf" in Fig. 4). The posttemporal foramen leads into the posttemporal canal between the two bones, which based on *Didelphis virginiana* (Wible 1990) and *Monodelphis domestica* (Wible 2003) transmits the arteria and vena diploëtica magna. On the lateral surface of the pars canalicularis, the canal is represented by the broad, sinuous posttemporal groove ("ptg" in Fig. 6A). Just anterior to the posttemporal foramen is a medially directed vascular canal ("vc" in Fig. 6A) that connects the posttemporal groove and the sulcus for the sigmoid sinus ("sss" in Fig. 7A) and is likely venous. Dorsal to the fossa incudis, the posttemporal groove narrows and joins the broad, dorsoventrally oriented sulcus for the prootic sinus ("sps" in Fig. 6A), which in turn has three exit routes. The largest is laterally into the suprameatal foramen ("smf" in Fig. 4), dorsal to external acoustic meatus, followed closely in size by a ventral exit into the postglenoid foramen ("pgf" in Figs. 2, 4), and the last is the small prootic canal mentioned above (Figs. 5A, 6A).

The endocranial surface of the petrosal is dominated by two large apertures: the larger anteromedially directed subarcuate fossa for the petrosal lobule of the cerebellum and ventral to it the medially directed internal acoustic meatus (Figs. 3, 7A). The former is on the pars canalicularis and the latter on the pars cochlearis ("pca" and "pco," respectively in Fig. 7A). The internal acoustic meatus is as wide as deep and its floor has a low transverse crest ("tc" in Fig. 7A). Anterior to the transverse crest is the foramen acusticum superius ("fas" in Fig. 7A), which contains the cribriform superior vestibular area dorsally and the facial canal ventrally. Posterior to the transverse crest is the foramen acusticum inferius ("fai" in Fig. 7A), which contains the spiral cribriform tract ventrally and the inferior vestibular area and foramen singulare dorsally. Forming the rim of the aperture into the subarcuate fossa is the anterior semicircular canal anteriorly and dorsally and the crus commune posteriorly ("asc" and "crc" in Fig. 7C). The aperture is constricted compared to the fossa lateral to it, but it is wider than the fossa is deep. In the posterodorsal floor of the subarcuate fossa is a small foramen that when followed in the CT scans joins the vascular canal connecting the posttemporal groove and the sulcus for the sigmoid sinus.

The endocranial surface has three substantial sulci for venous sinuses. The largest, the sulcus for the inferior petrosal sinus ("sips" in Fig. 7A), is on the posteromedial aspect of the pars cochlearis. The anteromedial aspect of the pars cochlearis has a deep concavity that contacts the basioccipital bone ("bof" in Fig. 7A). The smallest sulcus, for the superior petrosal sinus ("ssps" in Fig. 7A), runs on the anterior aspect of the pars canalicularis and onto the pars cochlearis opposite the foramen acusticum superius. The raised medial margin of this sulcus represents a rudimentary crista petrosa ("crp" in Fig. 7A) to which the tentorium cerebelli attached in life. The third sulcus, for the sigmoid sinus ("sss" in Fig. 7A), is on the dorsal aspect of the pars canalicularis and, as noted above, its primary outflow is onto a broad sulcus on the exoccipital (Fig. 3). At the posterior end of the sulcus for the sigmoid sinus is the opening into the vascular canal ("vc" in Fig. 7A) connecting to the posttemporal groove and subarcuate fossa.

The endocranial surface also has two openings associated with the endo- and perilymphatic systems. Dorsal to the jugular fossa ("jfo" in Fig. 7A), the petrosal's contribution to the jugular foramen, is the cochlear canaliculus ("cc" in Fig. 7A), which transmits the perilymphatic duct ("pld" in Figs. 7B–C). The cochlear canaliculus is a little longer than the long dimension of the round window. Posterodorsal to the cochlear canaliculus is the vestibular aqueduct ("va" in Fig. 7A), which transmits the endolymphatic duct ("end" in Figs. 7B–C). The endolymphatic duct connects to the saccule near the crus commune ("sac" and "crc" in Fig. 7C).

Auditory Elements.—The left osseous auditory elements of CM 110578, the ectotympanic, malleus, incus, stapes, and element of Paaw, are shown in articulation in Figure 8 and are described separately below. Table 1 includes volume

TABLE 1. Volume of isosurfaces of auditory elements rendered from CT scans of *Philander opossum*, CM 110578.

Bone	Volume (mm^3)
Element of Paaw (left)	0.062
Element of Paaw (right)	0.053
Stapes (left)	0.027
Stapes (right)	0.032
Incus (left)	0.128
Incus (right)	0.117
Malleus (left)	0.578
Malleus (right)	0.593
Ectotympanic (left)	1.919
Ectotympanic (right)	2.000

measurements of the individual elements. Perhaps the most striking result is that the element of Paaw has a larger volume than the stapes.

Ectotympanic.—The ectotympanic is a simple U-shaped bone that has contacts with two other basicranial bones: a small abutment ventrally with the alisphenoid tympanic process near the Glaserian fissure (Figs. 2, 4) and a more substantial abutment with the malleus along the anterior half of the ectotympanic (Fig. 8). The ectotympanic has a shallow sulcus malleolaris ("sm" in Figs. 9B–C) that accommodates the rostral (anterior) process of the malleus.

The legs of the U-shaped ectotympanic are the anterior crus and posterior crus ("acr" and "pcr," respectively in Fig. 9), and the broad gap separating the crura is the tympanic incisure, which in situ in the cranium is directed posterodorsally (Fig. 4). The crurae are only slightly expanded from a generally round profile. On the anterolateral surface near the midpoint between the crura is a low, rounded prominence, the styliform process ("sp" in Fig. 9A). It represents a remnant of the short third leg of the ectotympanic that is reported in early ontogenetic stages for *Didelphis marsupialis* Linnaeus, 1758 (Toeplitz 1920: taf. III, fig. 9) and *Monodelphis domestica* (Clark and Smith 1993: fig. 1B). The inner surface of the U has a sulcus that runs the length of the ectotympanic, the sulcus tympanicus ("st" in Fig. 9), for the attachment of the pars tensa of the tympanic membrane; the pars flaccida occupies the tympanic incisure. Based on the angulation of the ectotympanic, the pars tensa is at a near vertical angle in CM 110578: 82° as measured on section 666 in the transverse plane.

Malleus.—The malleus is the largest and most complex of the three auditory ossicles. It is anteroposteriorly elongate and mediolaterally compressed (Fig. 10) with a posterior contact with the incus and an anterior contact with the ectotympanic (Fig. 8).

The head of the malleus ("hm" in Fig. 10) is compressed and set off on its lateral surface by a distinct capitular crest that ends in a rounded capitular spine ("cc" and "cs," respectively in Fig. 10A). The head has two articular surfaces for the incus: the smaller inferior articular facet ("iaf" in Fig. 10D) is primarily convex, whereas the superior articular facet ("suaf" in Fig. 10D) is centrally convex and concave on its medial and lateral margins. The angle between the two facets is 100°. Inferior to the head is a distinct neck, which in turn is connected to the manubrial body ("nm" and "mb," respectively in Figs. 10A–B). On the medial surface of the neck is a low, barely raised process ("mp" in Fig. 10B) that we interpret as the attachment of the tensor tympani muscle. On the lateral surface of the manubrial body is a similarly low process that likely represents the lateral process ("lp" in Figs. 10A, D). Extending anteriorly from the manubrial body is the manubrium, which tapers to a point at its anterior end ("mn" in Fig. 10). Connecting the head, neck, and manubrial body is the thin osseous lamina ("ol" in Fig. 10A).

Extending anteriorly from the head is the thin, curved rostral (anterior) process ("rp" in Fig. 10A). Those didelphids for which ontogenetic stages have been studied (e.g., *Didelphis marsupialis*, Toeplitz 1920; *Monodelphis domestica* and *Caluromys philander* (Linnaeus, 1758), Sánchez-Villagra et al. 2002) show the usual mammalian pattern with the rostral process formed primarily by the gonial, a separate intramembranous ossification that fuses to the rest of the malleus, which is derived from Meckel's cartilage. At its anterior end, the rostral process expands into the tympanic plate ("tp" in Fig. 10). The dorsolateral and dorsomedial margins of the proximal rostral process have parallel crests, the outer and inner lamellae ("ola" and "ila," respectively in Figs. 10A–C). The outer lamella arises from the head, whereas the inner lamella arises from the osseous lamina. Between the two lamellae is the narrow intralamellar sulcus ("ils" in Fig. 10D), which accommodates the chorda tympani nerve, a branch of the facial nerve. The chorda tympani reaches the intralamellar sulcus by running in a groove on the medial surface of the osseous lamina ("gct" in Fig. 10B) and then into a short

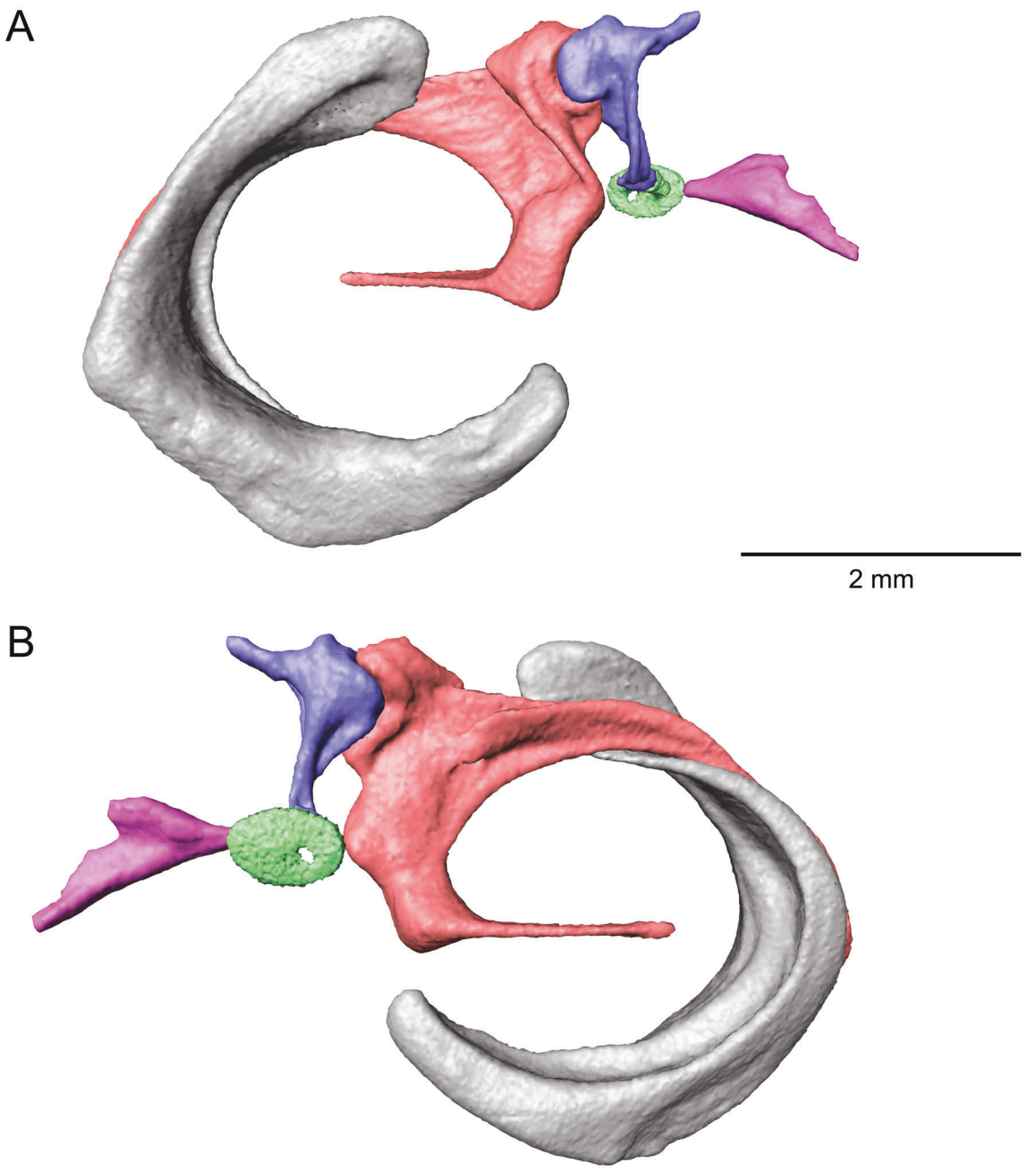

Fig. 8.—Isosurfaces rendered from CT data of left auditory apparatus of *Philander opossum*, CM 110578: **A,** lateral view; **B,** medial view. Ectotympanic = gray; incus = dark blue; malleus = red; stapes = green; element of Paaw = purple.

canal through the base of the inner lamella ("cct" in Figs. 10B–C).

Incus.—The incus has a broad articulation with the malleus and narrow one with the stapes (Fig. 8). It has a body and two arms, the long arm or crus longum and the short arm or crus breve ("bi," "cl," and "cb," respectively in Figs. 11A, C). The body is composed of two articular surfaces that contact the corresponding surfaces on the malleus: the superior and inferior articular surfaces ("sas" and "sis," respectively in Fig. 11B). Both are concave with the superior one convex on its medial and lateral margins. The crus longum is only slightly longer than the crus breve. Both the anterior and posterior surfaces of the crus longum are hollowed out producing a sulcus incudis ("si" in Fig. 11B); the sulcus on the posterior surface extends to the base of the crus breve. The distal end of the crus longum narrows and is bent medially as the pedicle ("ped" in Fig. 11B),

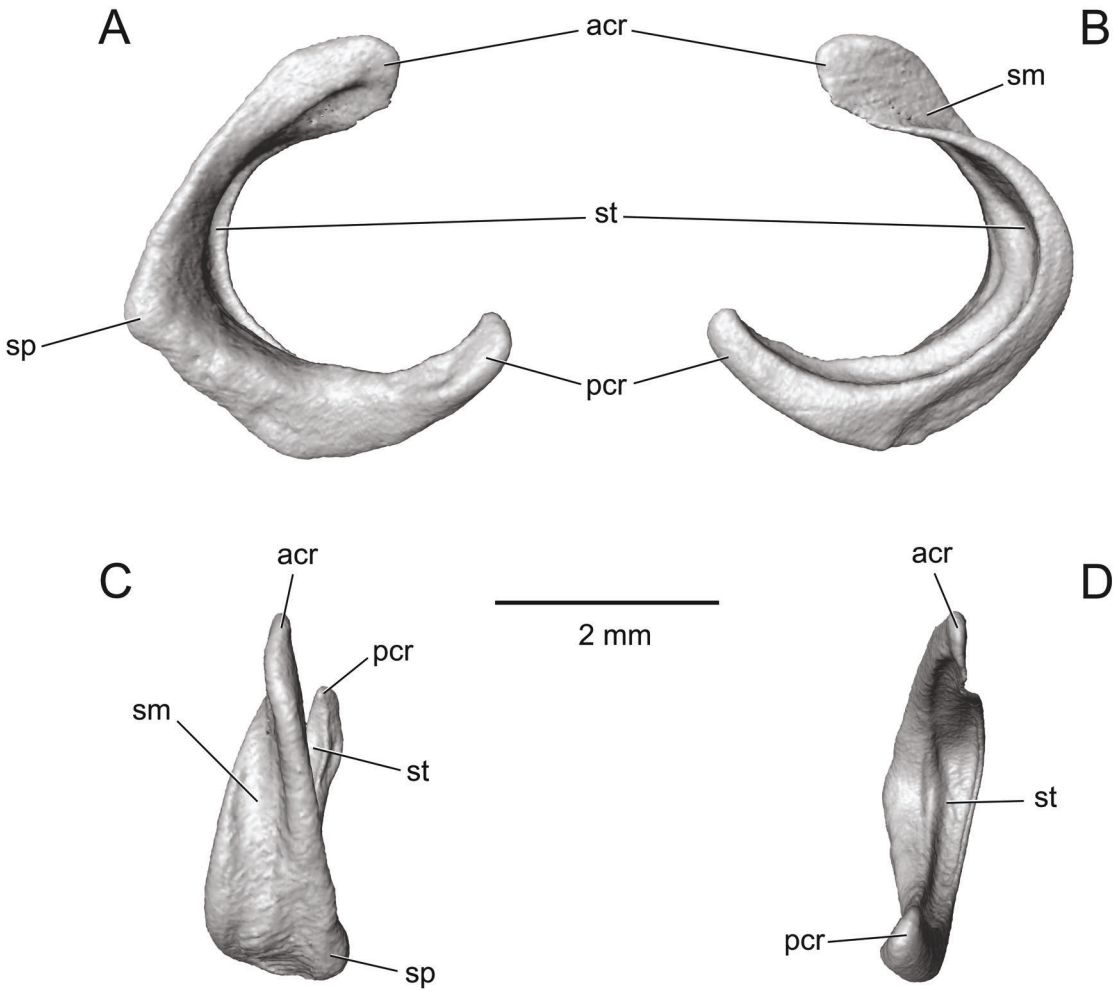

Fig. 9.—Isosurfaces rendered from CT data of left ectotympanic of *Philander opossum*, CM 110578: **A,** lateral view; **B,** medial view; **C,** anterior view; **D,** posterior view. Abbreviations: **acr,** anterior crus; **pcr,** posterior crus; **sm,** sulcus malleolaris; **sp,** styliform process; **st,** sulcus tympanicus.

which broadens into the disc-shaped lenticular process ("lpr" in Figs. 11B and C). The lenticular process articulates with the head of the stapes. The rod-like crus breve is set off from the crus longum at an angle of 70° and tapers distally to a point. It presumably has a ligamentous connection to the fossa incudis described with the petrosal above, but details of that connection cannot be obtained in our sample.

Stapes.—The stapes, the smallest auditory ossicle, articulates with the incus (Fig. 8) and is held in the fenestra vestibuli of the petrosal by the annular ligament. The stapes has a head, anterior and posterior crura, and a footplate ("hs," "acr," "pcr," and "fp," respectively in Figs. 11D–F). The two crura are rod-shaped, subequal, and separated by a narrow stapedial foramen ("stf" in Fig. 11F). The posterior crus has a prominent muscular process ("mps" in Figs. 11D, F) for the attachment of the stapedius muscle tendon. The footplate is oval with a small perforation near the anterior crus on the left stapes (Fig. 11E) that in life would be covered by connective tissue. The appearance of this small opening does not appear to be a threshold issue in the CT scans. The right stapes has no such perforation.

Element of Paaw.—The element of Paaw is not a simple nodule or rod shape but is triangular in medial and lateral views, with a long, straight ventral axis, a short, straight dorsal axis, and an irregular posterior axis (Figs. 11G–H). The anterior end of the element is rounded and attached to the stapedius muscle tendon, which is preserved bilaterally in CM 110578. The posterior half is embedded in the stapedius muscle, fibers of which are preserved bilaterally in CM 110574. The stapedius is a convergent muscle arising from the oval-shaped stapedius fossa on the pars canalicularis described above, and the fan-shape of the element of Paaw's posterior aspect reflects the shape of the stapedius

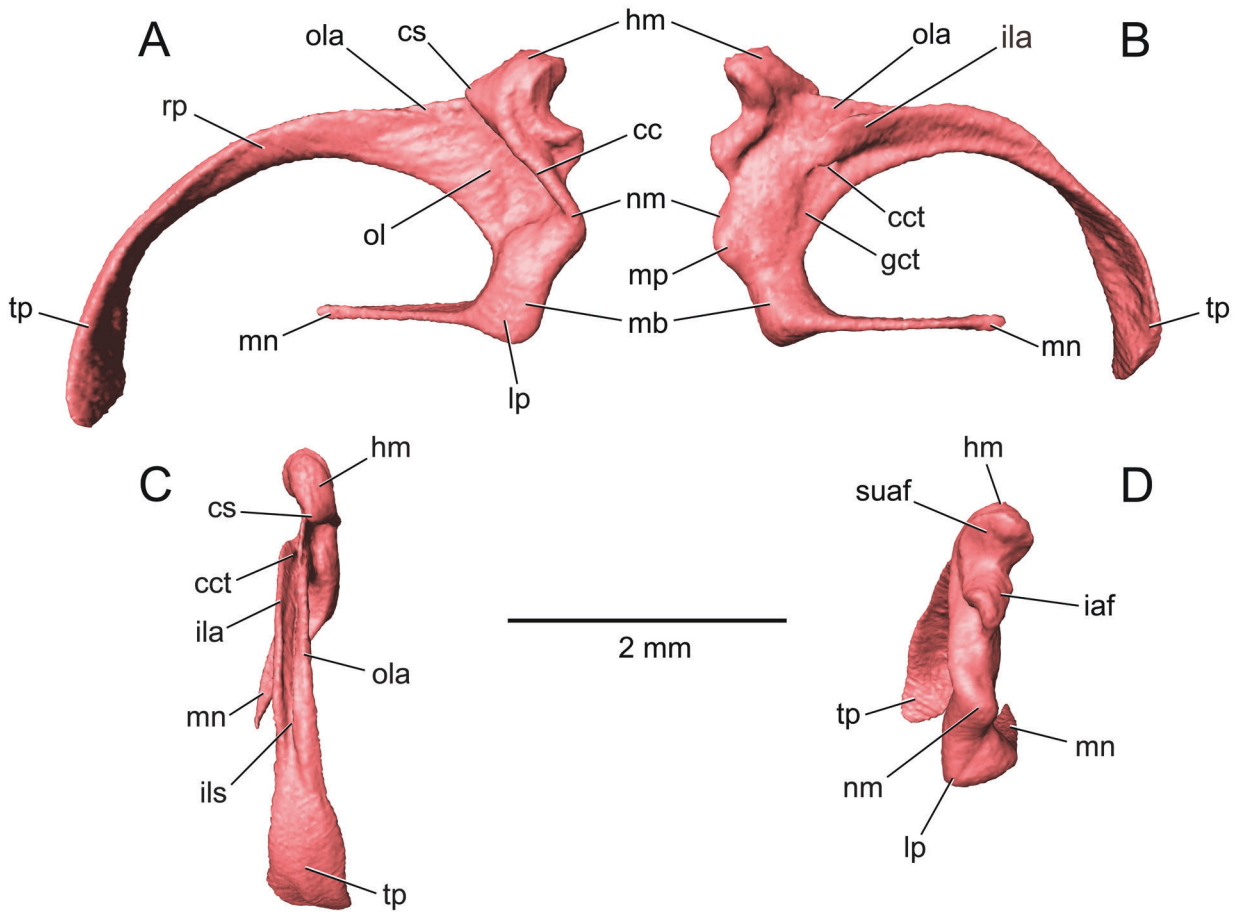

Fig. 10.—Isosurfaces rendered from CT data of left malleus of *Philander opossum*, CM 110578: **A,** lateral view; **B,** medial view; **C,** anterior view; **D,** posterior view. Abbreviations: **cc,** capitular crest; **cct,** canal for chorda tympani nerve; **cs,** capitular spine; **gct,** groove for chorda tympani nerve; **hm,** head; **iaf,** inferior articular facet; **ila,** inner lamella; **ils,** interlamellar sulcus; **lp,** lateral process; **mb,** manubrial base; **mn,** manubrium; **mp,** muscular process; **nm,** neck; **ol,** osseous lamina; **ola,** outer lamella; **rp,** rostral (anterior) process; **suaf,** superior articular facet; **tp,** tympanic plate of rostral process.

muscle. In ventral view (Fig. 5B), the element of Paaw is not straight but slightly curved with its medial aspect concave and lateral convex.

The shape and size of the element of Paaw differs slightly between the right and left sides of CM 110578. A cross section through the right bone shows that both medial and lateral surfaces are convex (see Fig. 12), but on the left side, the lateral surface is convex and the medial surface concave. The right element has a more irregular, spiny posterior border (Figs. 11G–J) and is also slightly smaller than the left (Table 1); the right bone is 89% the maximum length of the left.

Figure 12 shows four transverse sections from the CT scans of CM 110578: one through the fenestra vestibuli (Fig. 12A) and the others successively more posteriorly (Figs. 12B–D). The element of Paaw ("eP" in Figs. 12B–D) appears to have a density resembling that of the stapes and the crus breve ("s" and "cb," respectively in Fig. 12A). Given the adult status of the dentition of CM 110578, we anticipate that the stapes and incus are fully ossified, which suggests that the element of Paaw is as well. However, this should be treated as a working hypothesis.

Figures 12B–C show that the medial surface of the element of Paaw closely approximates the rear of the pars cochlearis, posterior to the fenestra vestibuli. Because the size of the gap between the two bones is comparable to that between the ventral ends of the squamosal and petrosal, which are in sutural contact in the skull, we accept that the element of Paaw and petrosal are in contact here. Review of the CT sections on both the right and left sides shows that this contact includes roughly the anterior fourth of the element. The ventral view of the element in situ on the petrosal (Fig. 5B) reveals that the narrow anterior part of the element passes dorsal to the bulge on the crista interfenestralis in the shallow sulcus described with the petrosal above (see also Fig. 12B), whereas the fan-shaped

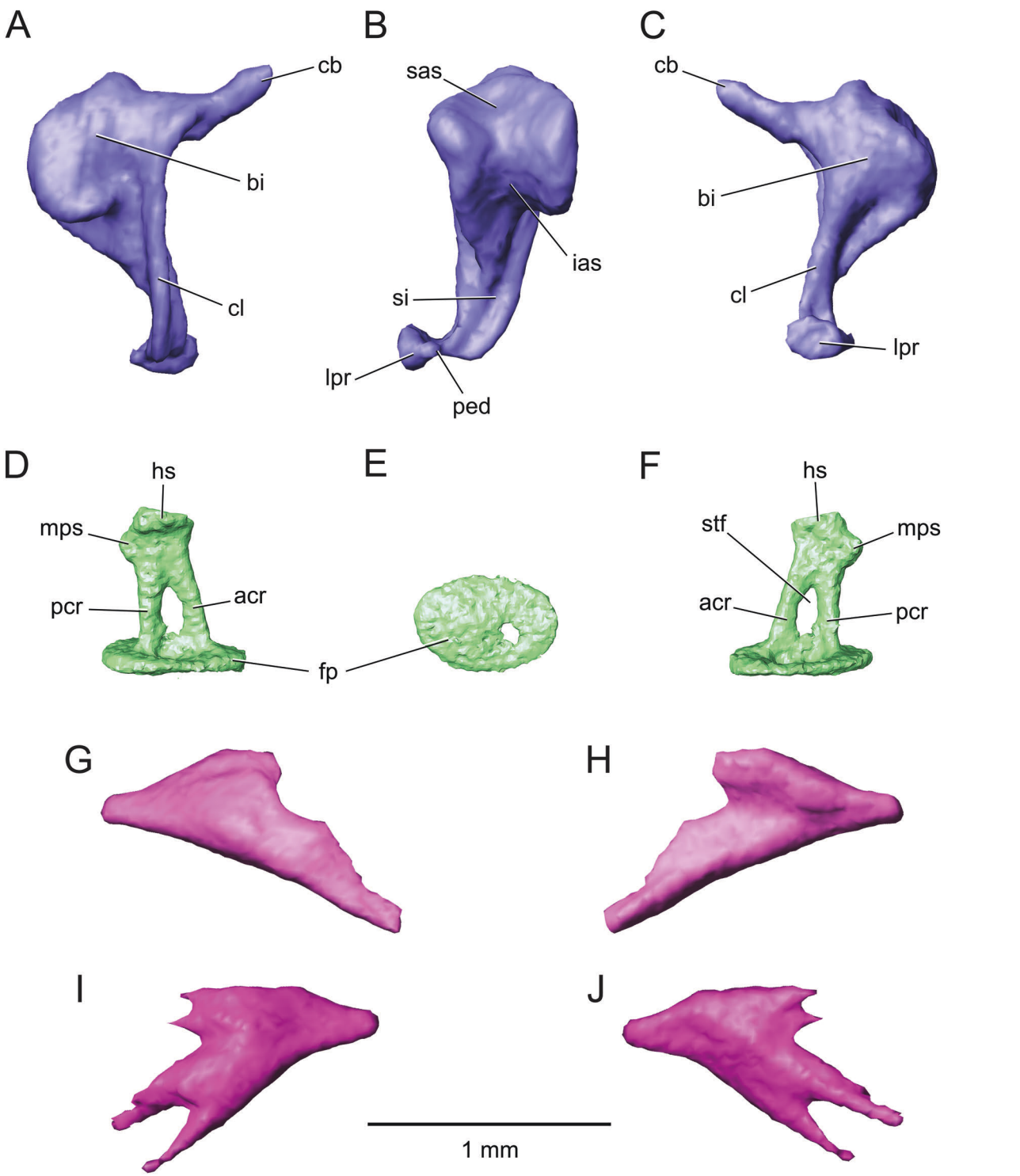

Fig. 11.—Isosurfaces rendered from CT data of *Philander opossum*, CM 110578: left incus in **A,** lateral, **B,** anterior, and **C,** medial views; left stapes in **D,** dorsal, **E,** medial, and **F,** ventral views; left element of Paaw in **G,** lateral and **H,** medial views; right element of Paaw in **I,** lateral and **J,** medial views. Abbreviations: **acr,** anterior crus of stapes; **bi,** body of incus; **cb,** crus breve; **cl,** crus longum; **fp,** footplate of stapes; **hs,** head of stapes; **ias,** inferior articular surface of incus; **lpr,** lenticular process of incus; **mps,** muscular process of stapes; **pcr,** posterior crus of stapes; **ped,** pedicle of incus; **sas,** superior articular surface of incus; **si,** sulcus incudis; **stf,** stapedial foramen.

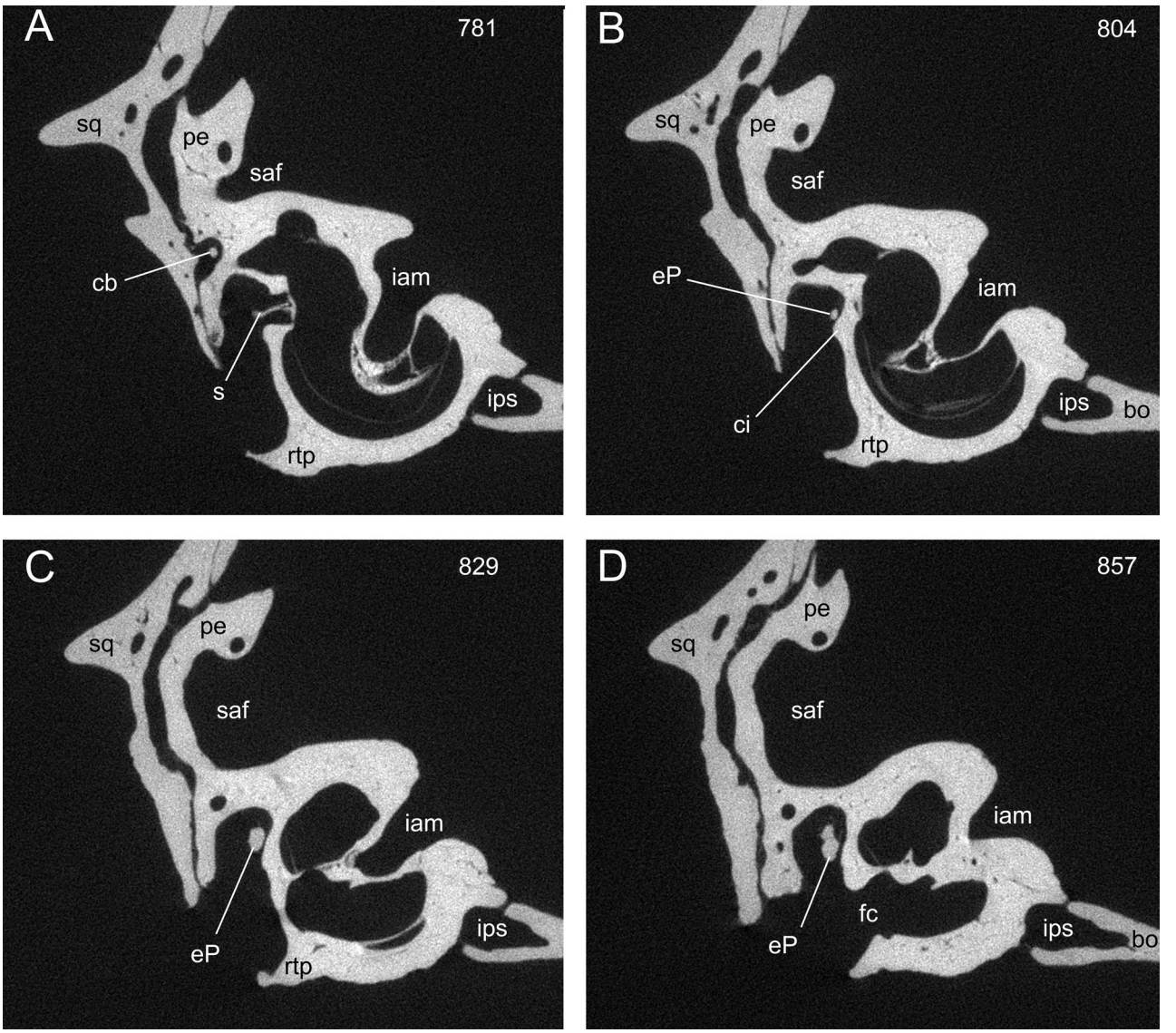

Fig. 12.—Transverse sections through the CT scan of the right ear region of *Philander opossum*, CM 110578. **A,** section 781 of 1400, through the fenestra vestibuli; **B,** section 804 of 1400, just posterior to the fenestra vestibuli; **C,** section 829 of 1400, more posterior to the fenestra vestibuli; **D,** section 857 of 1400, through the fenestra cochleae. Abbreviations: **bo,** basioccipital; **cb,** crus breve of incus; **ci,** bulge of crista interfenestralis; **eP,** element of Paaw; **fc,** fenestra cochleae; **iam,** internal acoustic meatus; **ips,** inferior petrosal sinus; **pe,** petrosal; **rtp,** rostral tympanic process; **s**, stapes; **saf,** subarcuate fossa; **sq,** squamosal.

posterior part is angled slightly medially towards the stapedius fossa. CM 110578 preserves connective tissue that attaches the narrow anterior part of the element to the pars cochlearis.

Petrosal of *Philander opossum* in Comparison to *Didelphis marsupialis* and *Monodelphis domestica*.—Rather than broad comparisons across Didelphidae, we chose to make remarks at a smaller scale by comparing *Philander opossum* with the two didelphids that the senior author has published on previously, *Didelphis* Linnaeus, 1758, and *Monodelphis* (Wible 1990, 2003; Wible and Hopson 1995). Our comparisons concern only a single CT scanned specimen for each taxon; consequently, any issues arising from intraspecific variation cannot addressed. We chose to focus on the petrosal bone given that the ectotympanic and auditory ossicles were not preserved in *Didelphis marsupialis*, DU BAA 0164, or did not provide the same level of detail in *Monodelphis domestica*, AMNH 261241, because of the lower resolution of the CT scans. Current views (e.g., Jansa et al. 2014) on the relationships of these three didelphids are that *Philander* Brisson, 1762, and *Didelphis* are sister taxa with a mean divergence time of 3.5 million years and *Monodelphis* is more distantly related with a mean divergence time from *Philander* and *Didelphis* of 19.9 million years.

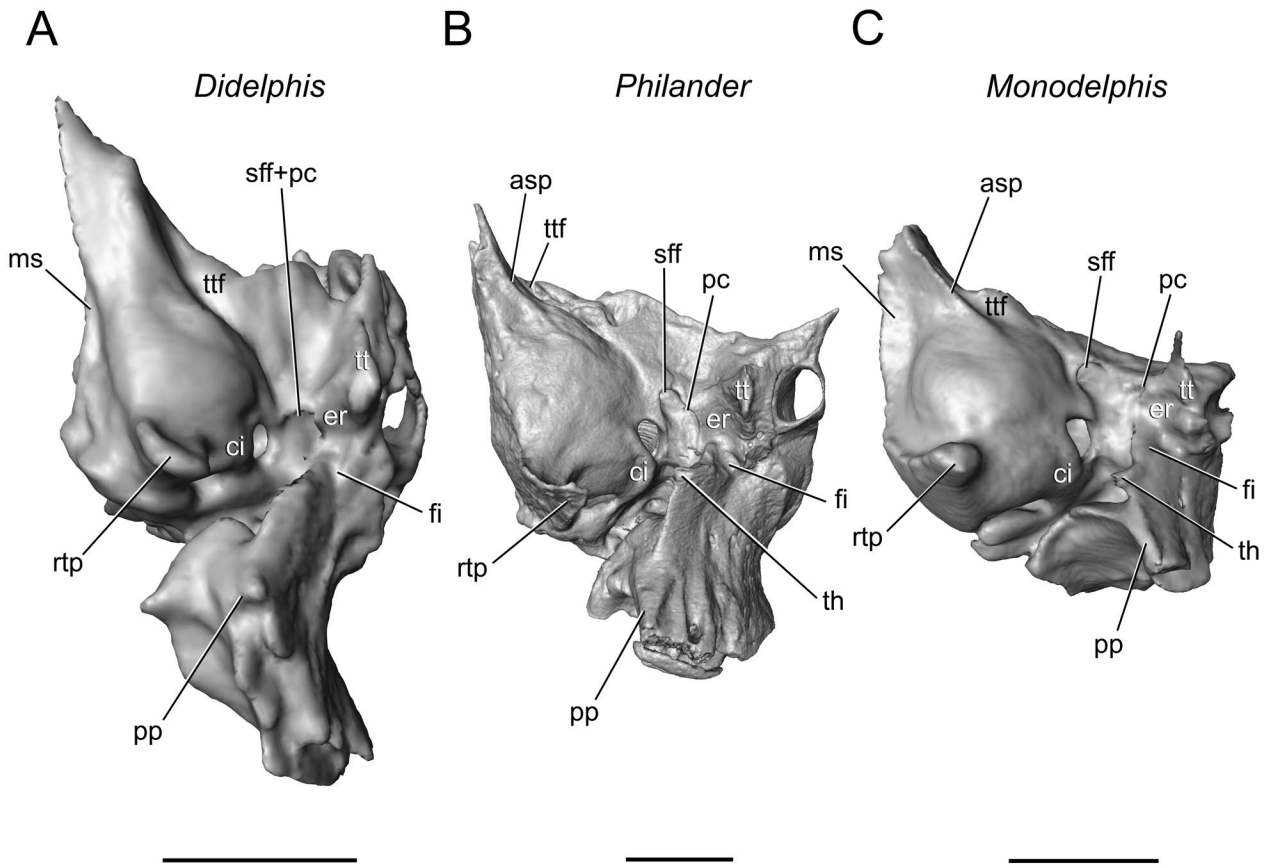

Fig. 13.—Isosurfaces rendered from CT data of left petrosals in ventral view. **A,** *Didelphis marsupialis*, DU BAA 0164; **B,** *Philander opossum*, CM 110578; **C,** *Monodelphis domestica*, AMNH 261241. Scale = 2 mm. Abbreviations: **asp,** anterior septum; **ci,** crista interfenestralis; **fi,** fossa incudis; **fs,** facial sulcus; **fv,** fenestra vestibuli; **ms,** medial shelf; **pc,** prootic canal; **pp,** paroccipital process; **rtp,** rostral tympanic process; **sff,** secondary facial foramen; **th,** tympanohyal; **tt,** tegmen tympani; **ttf,** tensor tympani fossa.

In ventral view (Fig. 13), the overall proportions and disposition of the pars cochlearis and par canalicularis are more similar in *Philander* and *Didelphis*; in *Monodelphis*, the pars canalicularis is compressed and does not extend far from the pars cochlearis. This is apparent, for example, by marking the relative distance between the promontorium and the paroccipital process. On the pars cochlearis, the rostral tympanic process is a simple process in all three, although *Philander* differs from the others in having a flat, plate-like process (Fig. 13B) rather than a digitiform one (Figs. 13A, C). In *Philander* and *Didelphis*, the rostral tympanic process is placed at the posteromedial aspect of the promontorium (Figs. 13A–B), whereas in *Monodelphis* it is more anteriorly positioned (Fig. 13C). Additionally, the rostral tympanic process in *Monodelphis* is continuous with a narrow medial shelf that extends nearly the length of the pars cochlearis (“ms” in Fig. 13C). A medial shelf occurs in *Didelphis* but it is not connected with the rostral tympanic process (Fig. 13A); *Philander* lacks a medial shelf. *Monodelphis* has a prominent anterior septum on the anteromedial pars cochlearis (“asp” in Fig. 13C); this ridge is present but faint in *Philander* (Fig. 13B) and absent in *Didelphis* (Fig. 13A). In *Monodelphis domestica* (Sanchez-Villagra and Forasiepi 2017: figs. 4c–d), the tensor tympani fossa is lateral to the anterior septum (“ttf” in Fig. 13C); *Didelphis* has the same configuration (Fig. 13A), but in *Philander* the fossa is very narrow (Fig. 13B). A feature where *Philander* resembles *Monodelphis* concerns the crista interfenestralis; in these two taxa, the crista is broad, thicker than the longest dimension of the oval and round windows (Figs. 13B–C), but in *Didelphis* the crista is narrower than the longest dimension (Fig. 13A). However, *Philander* is the only one with a prominent bulge on the crista interfenestralis; *Didelphis* and *Monodelphis* have a faint bulge with a faint sulcus dorsal to it interpreted for the element of Paaw.

On the pars canalicularis (Fig. 13), the position of the secondary facial foramen and the tympanic aperture of the prootic canal differ across the three taxa. In *Didelphis*, there is a common opening for both the secondary facial foramen and prootic canal anterolateral to the fenestra vestibuli (Fig. 13A); in *Philander*, the two openings are positioned farther from the fenestra vestibuli and separate but still connected by a ridge of bone between them (Fig.

13B); in *Monodelphis*, the two openings are fully separate and even farther from each other and the fenestra vestibui (Fig. 13C). The difference in position of these apertures affects the size of the floor beneath the cavum supracochleare, which is most extensive in *Didelphis* and barely present in *Monodelphis*. As noted by Sánchez-Villagra and Wible (2002: character 12), the position of the hiatus Fallopii is the same in these three taxa, with the floor and roof of the hiatus equal in length. The disposition of the areas on the pars canalicularis associated with the malleus and incus, the epitympanic recess and fossa incudis, is remarkably consistent across the three didelphids (Fig. 13). The epitympanic recess is a small space continuous posteriorly with the fossa incudis and with a low, longitudinal ridge on its lateral border representing the ventral aspect of the tegmen tympani. The tegmen tympani of *Monodelphis* differs in that it ends anteriorly as a very narrow prong (Fig. 13C); this was not the case in the isolated petrosal of *Monodelphis* sp. illustrated by Wible (2003: figs. 7A, C), which either represents variation or possible breakage. *Philander* and *Monodelphis* have a distinct tympanohyal on the crista parotica (Figs. 13B–C); this is absent in *Didelphis* (Fig. 13A).

In lateral view (Fig. 14), the major differences concern features of the vascular system. All three taxa have a well-developed sulcus transmitting the prootic sinus ventrally toward the postglenoid and suprameatal foramina in the squamosal as well as the diminuitive lateral aperture of the prootic canal in the petrosal. However, *Philander* and *Didelphis* differ from *Monodelphis* in that the petrosal encloses the sulcus to produce a foramen for the prootic sinus that is positioned dorsal to these three exit points. Such a foramen has not been identified previously in isolated petrosals of either *Didelphis* or *Philander* (e.g., *Didelphis virginiana*, Wible 1990: fig. 4; *Philander opossum*, Sánchez-Villagra and Wible 2002: fig. 3a), which we cannot currently judge as absence due to breakage of relatively delicate structures or absence due to true variation. The other difference concerns the extent of the posttemporal groove; in *Philander* and *Didelphis*, it extends from the mastoid exposure to the sulcus for the prootic sinus (Figs. 14A–B), but in *Monodelphis*, it is only present as a small indentation at the site of the posttemporal foramen on the mastoid exposure (Fig. 14C). The absence of a posttemporal groove was also noted for isolated petrosals of *Monodelphis* sp., CM 5024, by Wible (2003). In contrast, Sánchez-Villagra and Wible (2002: character 13) reported the posttemporal groove as present in *Monodelphis* sp., AMNH 133248, even though their illustration (2002: fig. 5d) does not show it as present.

In dorsomedial view (Fig. 15), the size and shape of the internal acoustic meatus differ across the three taxa. In *Didelphis*, the meatus is circular and is much deeper than it is wide (Fig. 15A); in *Philander*, it is oval and as wide as deep (Fig. 15B); and in *Monodelphis*, it is oval and much wider than deep (Fig. 15C). The aperture of the internal acoustic meatus is about the same width as the aperture of

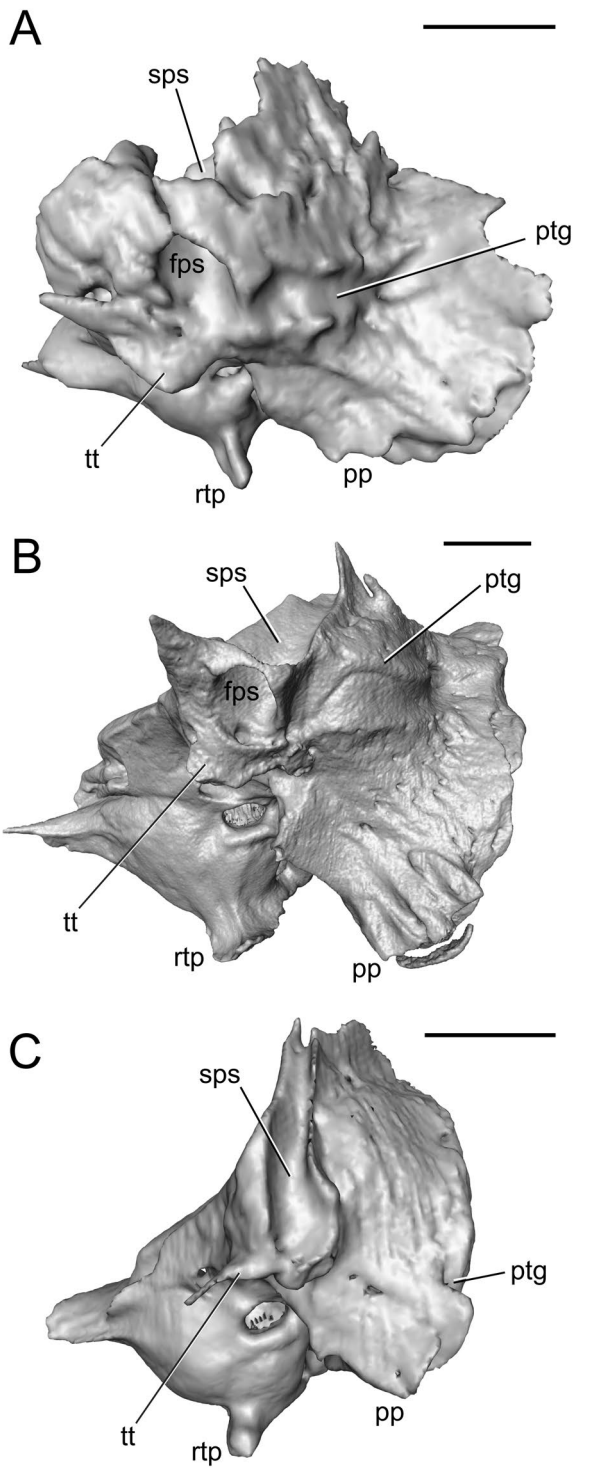

Fig. 14.—Isosurfaces rendered from CT data of left petrosals in lateral view. **A,** *Didelphis marsupialis*, DU BAA 0164; **B,** *Philander opossum*, CM 110578; **C,** *Monodelphis domestica*, AMNH 261241. Scale = 2 mm. Abbreviations: **fps,** foramen for prootic sinus; **pp,** paroccipital process; **ptg,** posttemporal groove; **rtp,** rostral tympanic process; **sps,** sulcus for prootic sinus; **tt,** tegmen tympani.

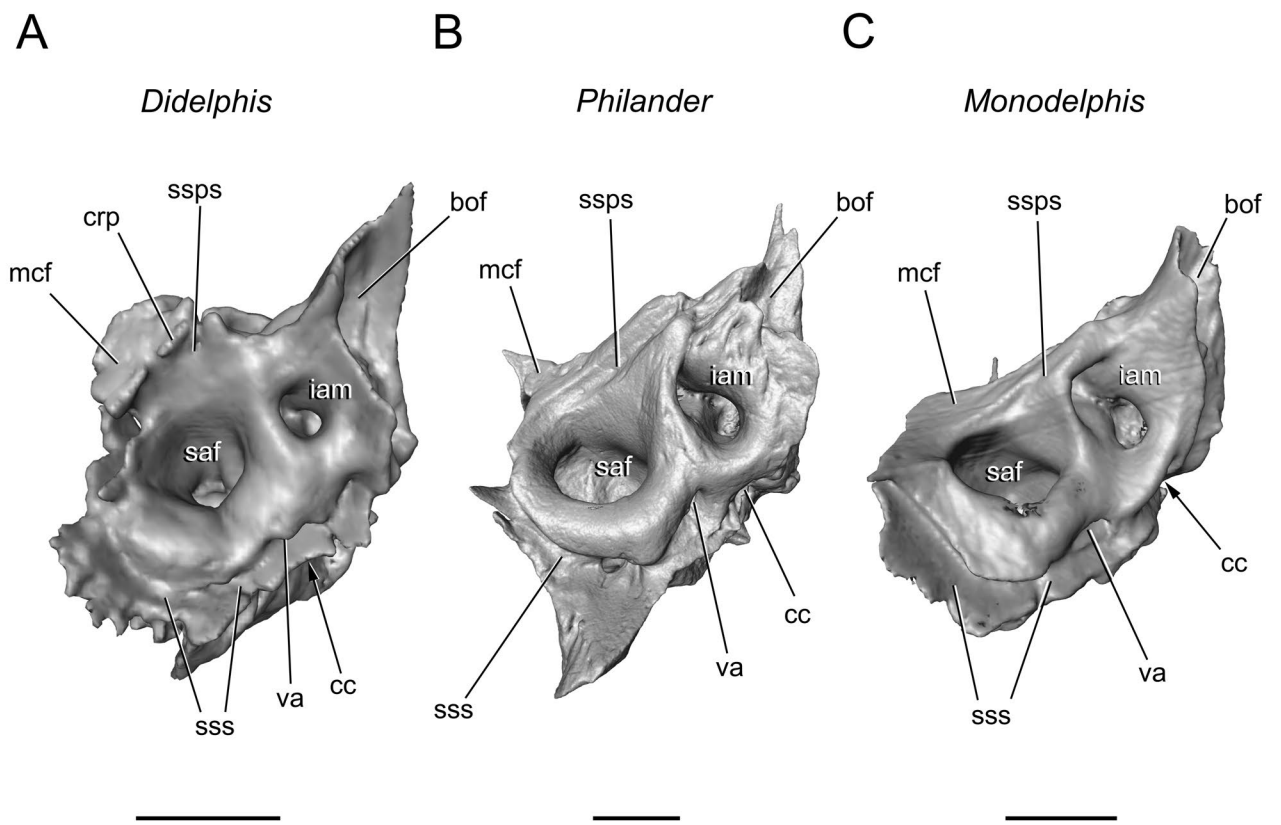

Fig. 15.—Isosurfaces rendered from CT data of left petrosals in dorsomedial view. **A,** *Didelphis marsupialis*, DU BAA 0164; **B,** *Philander opossum*, CM 110578; **C,** *Monodelphis domestica*, AMNH 261241. Scale = 2 mm. Abbreviations: **bof,** basioccipital facet; **cc,** cochlear canaliculus; **crp,** crista petrosa; **iam,** internal acoustic meatus; **mcf,** bone exposed in middle cranial fossa; **saf,** subarcuate forra; **sips,** sulcus for inferior petrosal sinus; **ssps,** sulcus for superior petrosal sinus; **sss,** sulcus for sigmoid sinus; **va,** vestibular aqueduct.

the subarcuate fossa in *Monodelphis* (Fig. 15C), is slightly smaller in *Philander* (Fig. 15B), and is much smaller in *Didelphis* (Fig. 15A). In *Didelphis*, the aperture of the subarcuate fossa is the widest part of the recess (Fig. 15A), but in *Philander* and *Monodelphis*, the aperture is constricted compared to the fossa (Figs. 15B–C). Also, the subarcuate fossa is deeper than wide in *Didelphis* but wider than deep in *Philander* and *Monodelphis*. All three have a sulcus for the superior petrosal sinus anterolateral to the subarcuate fossa (Fig. 15), but only *Didelphis* has a raised crista petrosa forming the anterior edge of that sulcus (Fig. 15A). Each has a small area anterior to the sulcus for the superior petrosal sinus that is exposed in the middle cranial fossa (Fig. 3), although this is more substantial in *Didelphis* (Fig. 15A) than in the other two (Figs. 15B–C). In *Philander* (Fig. 3) and *Didelphis*, the anterior edge of this area contacts the squamosal bone in the middle cranial fossa, but in *Monodelphis*, it is separated from contact with the squamosal by the parietal and alisphenoid. All three have a sulcus for the sigmoid sinus. In *Didelphis* (Fig. 15A) and *Monodelphis* (Fig. 15C), it is both dorsal and posterior to the subarcuate fossa; however, in the former it has a foramen magnum exit via a sulcus in the exoccipital (see also Dom et al. 1970), whereas in the latter its exit is the jugular foramen. In *Philander* (Fig. 15B), the sulcus is only dorsal to the subarcuate fossa and exits via the foramen magnum (Fig. 3). The vestibular aqueduct for the endolymphatic duct is in essentially the same position in all three, but the cochlear canaliculus for the perilymphatic duct differs. In *Didelphis*, it is proximate to the vestibular aqueduct but in the jugular fossa and not within the endocranium (Fig. 15A). In *Monodelphis*, the cochlear canaliculus is widely separated from the vestibular aqueduct and within the endocranium (Fig. 15C). *Philander* is intermediate, with some separation between the two (Fig. 15B) and the cochlear canaliculus at the juncture of the endocranium and jugular fossa. Finally, each has a deep concavity along the anteromedial aspect of the pars cochlearis that represents a facet for the basioccipital ("bof" in Fig. 15). In *Monodelphis* this facet is about one-third the length of the pars cochlearis, whereas it is half the length in *Philander* and *Didelphis*.

Auditory Ossicle Characters in *Philander opossum*.— Schmelzle et al. (2005) reported the distribution of 13 characters of the auditory ossicles across 31 species of

extant marsupials, including *Philander opossum* based on CM 4995. Given how little we know about possible variation, we compare our findings for *Philander opossum*, CM 110578, with those in Schmelzle et al. (2005) for CM 4995. Unfortunately, there are no ossicles currently preserved with CM 4995, which means we cannot verify the prior observations.

Our observations on CM 110578 are congruent with those of Schmelzle et al. (2005) in the following: character 1, the superior articular facet of the malleus is longer than the inferior (Fig. 10D); character 2, the distal end of the manubrium is not spatulated (Figs. 10A–B); character 6, the crus longum is gracile (Figs. 11A–C); character 7, the angle between the crus longum and crus breve is greater than 90 degrees (Figs. 11A, C); Character 8, the incus sulcus is present (Fig. 11B); character 10, the ventral surface of the crus breve is smooth (Figs. 11A, C); character 12, the stapes is bicrurate and not columelliform (Figs. 11D, F); and character 13, the stapes base (footplate) is flat (Figs. 11D, F). Schmelzle et al. (2005: character 11) scored the stapedial ratio for *Philander opossum* as less than 1.8, which we found for CM 110578 (Table 4), but following the ratios published in Horovitz et al. (2008) based on more specimens, this taxon should be scored polymorphic, both below and above 1.8.

Our observations on CM 110578 differ from those of Schmelzle et al. (2005) in the following: character 3, the angle between the manubrium and manubrial base is more than 100 degrees in CM 110578 (Figs. 10A–B) (see also CM 52731 and 69803) but was reported as approximately a right angle in Schmelzle et al. (2005); character 4, the neck of the malleus projects beyond the manubrial base in CM 110578 (Figs. 10A–B) (see also CM 52731 and 69803), but was reported as not projecting in Schmelzle et al. (2005); character 5, the manubrium is straight in CM 110578 (Figs. 10A–B) (see also CM 52731 and 69803), but was reported as curved in Schmelzle et al. (2005); and character 9, the dorsal surface of the incus appears even in CM 110578 (Figs. 11A, C) (see also CM 52731 and 69803) but was reported as grooved in Schmelzle et al. (2005). These discrepancies may relate to differences in the interpretation of the characters and states; Schmelzle et al. (2005) did not provide measurement guides and the differences between the grooved and smooth states for the dorsal surface of the incus appear subtle (compare *Bettongia penicillata* in fig. 4 and *Spilocuscus maculatus* in fig. 5 in Schmelzle et al. 2005).

Observations of the Element of Paaw from the Literature

In his summary of the literature to date, Klaauw (1923) recorded a cartilaginous and/or osseous element of Paaw in representatives of the following therian orders (# of genera): Didelphimorphia (1), Diprodontia (2), Cingulata (4), Pilosa (3), Primates (1), Scandentia (1), Dermoptera (1), Artiodactyla (3), Perissodactyla (2), Chiroptera (1), Pholidota (2), and Erinaceomorpha (1). In Table 2, the post-1923 instances of an element of Paauw in the literature are added to those in Klaauw (1923). Table 2 includes two placental orders not in Klaauw (1923): Rodentia and Carnivora, each with two genera. In addition, our literature review increased the number of genera in four orders as follows: Didelphimorphia (+2), Diprotodontia (+1), Scandentia (+1), and Chiroptera (+12). None of these observations from the literature include precise information on size, shape, or position, and there are few illustrations of the entire bone/cartilage.

A few orders have conflicting observations. In Scandentia, an element of Paaw is reported in adult *Tupaia* Raffles, 1821, by Hinchcliffe and Pye (1969) and Wible (2009) but was not found in prenatal stages by Spatz (1964), MacPhee (1981), and Zeller (1983). In Erinaceomorpha, Parker (1885b) reported an element in *Erinaceus europaeus* Linnaeus, 1758, but Henson (1961) and MacPhee (1981) specifically noted its absence. The only reported instance in Primates is in *Homo sapiens* Linnaeus, 1758, based on several old anatomical texts as summarized by Klaauw (1923; see also Graboyes et al. 2011a). One of these, "Quain's Elements of Anatomy" (Sharpey et al. 1878: 638), stated "A very slender spine of bone has been found occasionally in the tendon of the stapedius in man: and a similar piece of bone, though of a rounder shape, exists constantly in the horse, the ox, and other animals." This is also noted in "Rauber's Lehrbuch der Anatomie des Menschen" (Kopsch 1909: 194) but we have not found similar observations in subsequent textbooks of human anatomy (e.g., Jackson 1914; Robinson 1921). Graboyes et al. (2011a: 1187) stated "To the authors' knowledge, there is no current evidence for an ossicle of Paaw in humans." However, there are reports in humans of congenital ossification of the stapedius tendon resulting in hearing loss correctable by surgery (e.g., Kurosaki et al. 1995; Carmino and Blanco 2018). The description of this abnormality resembles that above by Sharpey et al. (1878), which makes us wonder if that malformation was being reported in old anatomical texts.

In their paper on the distribution of sesamoid bones in tetrapods, Abdala et al. (2019: table 1) noted the presence of the cartilage of Paaw among mammals in Marsupialia, Carnivora, Primates, and Rodentia, citing Hinchcliffe and Pye (1969). Obviously, this does not cover all the higher-level diversity noted by Klaauw (1923). Moreover, the inclusion of Primates by Abdala et al. (2019) is in error. Hinchcliffe and Pye (1969) included one observation in Primates, that in *Tupaia*, and on one side only in one specimen. In 1969, treeshrews were considered to be members of Primates (e.g., Napier and Napier 1967), but they are now placed in their own order Scandentia (Wilson and Reeder 2005). Other than the controversial element reported in humans, an element of Paaw is unknown in Primates.

TABLE 2. Reports of cartilaginous or osseous element of Paaw in the literature.
(*continued on following page*)

Order	Family	Taxon	Age	Composition	Term Used	Reference
Didelphimorphia	Didelphidae	*Caluromys philander*	newborn	cartilage	cartilage of Paauw	Sánchez-Villagra et al. 2002
Didelphimorphia	Didelphidae	*Caluromys philander*	pouch young	cartilage	cartilage of Paauw	Sánchez-Villagra et al. 2002
Didelphimorphia	Didelphidae	*Didelphis virginiana*	pouch young	cartilage then bone	Paauw's cartilage	McClain 1939
Didelphimorphia	Didelphidae	*Monodelphis brevicaudata*	adult	bone	element of Paaw	Wible 2003
Didelphimorphia	Didelphidae	*Monodelphis domestica*	prenatal day 12, 30, newborn, pouch young	cartilage then bone	cartilage of Paauw	Sánchez-Villagra et al. 2002
Didelphimorphia	Didelphidae	*Monodelphis domestica*	pouch young	cartilage	Paauw's cartilage	Filan 1991
Didelphimorphia	Didelphidae	*Monodelphis domestica*	pouch young	cartilage	element of Paaw	Sánchez-Villagra & Forasiepi 2017
Diprotodontia	Macropodidae	*Macropus eugenii*	pouch young	cartilage	element of Paaw	Sánchez-Villagra & Forasiepi 2017
Diprotodontia	Macropodidae	*Macropus rufogriseus*	pouch young	cartilage	element of Paaw	Sánchez-Villagra et al. 2002
Diprotodontia	Phalangeridae	*Trichosurus vulpecula*	adult	bone	not named	Hyrtl 1845
Diprotodontia	Vombatidae	*Vombatus ursinus*	adult	bone	not named	Hyrtl 1850
Cingulata	Dasypodidae	*Dasypus hybridus*	embryo	cartilage	interhyal	Parker 1885a
Cingulata	Dasypodidae	*Dasypus hyfridus*	adult	bone	element of Paaw	Basso et al. 2020
Cingulata	Dasypodidae	*Dasypus novemcinctus*	adult	bone	not named	Hyrtl 1845
Cingulata	Dasypodidae	*Dasypus novemcinctus*	adult	bone	cartilage of Paaw	Wible 2010
Cingulata	Chlamyphoridae	*Chaetophractus vellerosus*	adult	bone	element of Paaw	Basso et al. 2020
Cingulata	Chlamyphoridae	*Chaetophractus villosus*	embryo	cartilage	interhyal	Parker 1885a
Cingulata	Chlamyphoridae	*Chaetophractus villosus*	adult	bone	element of Paaw	Basso et al. 2020
Cingulata	Chlamyphoridae	*Priodontes maximus*	adult	bone	not named	Hyrtl 1845
Cingulata	Chlamyphoridae	*Cabassous unicinctus*	adult	bone	not named	Hyrtl 1845
Pilosa	Choloepodidae	*Choloepus didactylus*	embryo	cartilage	interhyal	Parker 1885a
Pilosa	Myrmecophagidae	*Cyclopes didactylus*	embryo	cartilage	interhyal	Parker 1885a
Scandentia	Ptilocercidae	*Ptilocercus lowii*	adult	bone	element of Paaw	Wible 2009
Scandentia	Tupaiidae	*Tupaia glis*	adult	bone	element of Paaw	Wible 2009
Scandentia	Tupaiidae	*Tupaia* sp.	?	bone	not named	Hyrtl 1845
Dermoptera	Cynocephalidae	*Cynocephalus volans*	adult	?	interhyal	Parker 1885b
Rodentia	Heteromyidae	*Microdipodops pallidus*	adult	cartilage	Paaw's cartilage	Hinchcliffe & Pye 1969

TABLE 2. Reports of cartilaginous or osseous element of Paaw in the literature.
(*continued from previous page*)

Order	Family	Taxon	Age	Composition	Term Used	Reference
Rodentia	Cricetidae	*Oryzomys laticeps*	adult	cartilage	Paaw's cartilage	Hinchcliffe & Pye 1969
Artiodactyla	Bovidae	*Bos taurus*	adult	bone	not named	Hyrtl 1845; Chauveau 1871
Artiodactyla	Bovidae	*Ovis aries*	adult	bone	not named	Chauveau 1871
Artiodactyla	Suiidae	*Sus scrofa*	embryo; newborn	cartilage	interhyal	Parker 1874
Perissodactyla	Tapiridae	*Tapir terrestris*	adult	bone	not named	Hyrtl 1845
Perissodactyla	Equidae	*Equus caballus*	adult	bone	not named	Chauveau 1871
Chiroptera	Molossidae	*Molossus ater*	adult	?	Paauw's cartilage	Pye 1966
Chiroptera	Molossidae	*Molossus coebensis*	adult	?	Paauw's cartilage	Pye 1966
Chiroptera	Molossidae	*Molossus major*	adult	?	Paauw's cartilage	Pye 1966
Chiroptera	Molossidae	*Tadarida brasiliensis*	adult	cartilage	skeletal element of Paauw	Henson 1961
Chiroptera	Natalidae	*Natalus mexicanus*	adult	bone	skeletal element of Paauw	Henson 1961
Chiroptera	Natalidae	*Natalus tumidirostris*	adult	cartilage	Paaw's cartilage	Hinchcliffe & Pye 1969
Chiroptera	Phyllostomidae	*Anoura geoffroyi*	adult	cartilage	Paaw's cartilage	Hinchcliffe & Pye 1969
Chiroptera	Phyllostomidae	*Artibeus jamaicensis*	adult	cartilage	Paaw's cartilage	Hinchcliffe & Pye 1969
Chiroptera	Phyllostomidae	*Chiroderma villosum*	adult	cartilage	Paaw's cartilage	Hinchcliffe & Pye 1969
Chiroptera	Phyllostomidae	*Glossophaga soricina*	adult	cartilage	skeletal element of Paauw	Henson 1961
Chiroptera	Phyllostomidae	*Platyrrhinus helleri*	adult	cartilage	Paaw's cartilage	Hinchcliffe & Pye 1969
Chiroptera	Rhinolophidae	*Rhinolophus ferrum-equinum*	adult	cartilage	skeletal element of Paauw	Henson 1961
Chiroptera	Rhinopomatidae	*Rhinopoma microphyllum*	adult	cartilage	not named	Bondy 1907
Chiroptera	Vespertilionidae	*Eptesicus fuscus*	adult	bone	skeletal element of Paauw	Henson 1961
Chiroptera	Vespertilionidae	*Myotis albescens*	adult	?	Paauw's cartilage	Pye 1966
Chiroptera	Vespertilionidae	*Myotis myotis*	adult	bone	os quartum; cartilage of Paaw	Cabezudo et al. 1983
Chiroptera	Vespertilionidae	*Pipestrellus pipestrellus*	adult	?	Paauw's cartilage	Pye 1966
Carnivora	Nandiniidae	*Nandinia binotata*	adult	bone	cartilage of Paauw	Wible & Spaulding 2013

Observations of the Element of Paaw from Digital Morphology at the University of Texas at Austin

Table 3 shows the specimens of extant mammals with coronal slice movies on DigiMorph.org where we observed an element of Paaw, bilaterally in most instances. The element is present in 15 of the 37 marsupial specimens studied (see Appendix 1) and in one of the 169 placental specimens, but is absent in the four monotreme specimens. We note that these movies are not all of the same resolution and that our failure to observe an element of Paaw may be the result of the difference in resolution. Given the circumstances of the data available in these slice movies, we did not attempt to measure the element. We assume that the structure in question is osseous as it appears to be similar in density to neighboring bone, but cannot confirm this. Additionally, the element of Paaw had some contact with the pars cochlearis in the majority of these movies; the exceptions were the 27 and 90 day-old *Monodelphis domestica*, *Cercartetus caudatus* (Milne-Edwards, 1877), and *Petauroides volans* Thomas, 1888, where a narrow gap separates the two bones. Table 3 adds significantly to the diversity of marsupials with an element of Paaw, including representatives of all orders except Notoryctemorphia, adding Paucituberculata (1 genus), Microbiotheria (1 genus), Dasyuromorphia (1 genus), and Peramelemorphia (2 genera) to what was known previously (Table 2). It also adds another genus of Didelphimorphia and two of Diprotodontia.

The lone placental found with an element of Paaw was the nine-banded armadillo, *Dasypus novemcinctus* Linnaeus, 1758; it also had the element in contact with the pars cochlearis. The cartilage of Paaw has been reported previously in prenatal *D. novemcinctus* by Reinbach (1952a, b) and an ossified element of Paaw in adults by Hyrtl (1845) and Wible (2010).

Observations of the Element of Paaw from CT Scanned Specimens from MorphoSource.org

The CT scan data for the nine marsupials downloaded from MorphoSource.org (Appendix 2) revealed the bilateral presence of an element of Paaw, except for *Didelphis marsupialis*, in which the element was preserved only on the left side. We considered the elements to be osseous as they appear similar in density to neighboring bone. Table 4 includes measurements of the element, the stapedial footplate, and skull length for these nine specimens plus *Philander opossum*, CM 110578. The element is a substantial structure that is longer than the long axis of the stapedial footplate, except in the caenolestid *Rhyncholestes raphanurus* Osgood, 1924, where the element is 70% the length of the footplate. An element of Paaw longer than the footplate occurs in representatives of four orders, Didelphimorphia, Microbiotheria, Peramelemorphia, and Notoryctemorphia.

The element of Paaw is a straight rod in eight of the nine marsupial specimens; the exception is *Notoryctes typhlops* (Stirling, 1889), which has a triangular outline reminiscent of that in *Philander opossum*, CM 110578, although it is straight and not bent as in the latter. In those with a rod shape, the element tapers anteriorly in *Caluromys* sp., *Caluromysiops irrupta* Sanborn, 1951, *Didelphis marsupialis*, *Didelphis* sp., and *Monodelphis domestica*, tapers posteriorly in *Rhyncholestes raphanurus* and *Isoodon obesulus* (Shaw, 1797), and is uniform in *Dromiciops gliroides* Thomas, 1894. As described above in *Philander opossum*, CM 110578, the anterior end of the element contacts the pars cochlearis posterior to the fenestra vestibuli in five of the nine marsupials. In the four lacking such contact, there is a slight gap between the two bones in *Caluromys* sp. and *Monodelphis domestica*, the element is fully divorced from the petrosal, in *Notoryctes typhlops*, and the element has been shifted in position in *Didelphis marsupialis* given that the long axis of the one preserved element is mediolateral rather than anteroposterior.

We also captured data on the shape of the stapedial footplate, which occupies the fenestra vestibuli, by calculating the stapedial ratio (of Segall 1970; length/width of the footplate). The ratios (Table 4) range from a low of 1.40 in *Notoryctes typhlops* to a high of 2.07 in *Caluromysiops irrupta*.

Observations of the Element of Paaw from Carnegie Museum of Natural History Specimens

Table 5 lists species of marsupials in the collections of the Carnegie Museum of Natural History in which an element of Paaw was found in some representatives. This includes representatives of all 27 species of Didelphidae in the collection along with three Dasyuridae, one Peramelidae, and one Vombatidae. In Table 5, we report the number of specimens of each of these 32 species that we examined and the percentage that had no element of Paaw, the element on one side only, and the element on both sides. Fifteen species had 100% bilateral incidence in the specimens examined. The largest sample was *Didelphis virginiana*, with 100 specimens of which 37 had bilateral elements, 24 had one element, and 39 had no element. We did not attempt to measure the element of Paaw as the extent of visual access to the bone varies considerably across the sampled taxa. Our general impression is that the element is generally at least as long as the stapedial footplate or fenestra vestibuli.

Table 6 lists the 17 species of marsupials in the CM collection for which we were unable to observe an element of Paaw. The vast majority of these have a complete or nearly complete osseous bulla, which obscures view of the area where the element of Paaw would be expected. There were only three species with specimens that we could confirm the absence of the element of Paaw: *Thylacinus cynocephalus* (Harris, 1808), CM 20975, *Phascolartos cinereus* (Goldfuss, 1817), CM 20928, and *Tarsipes rostratus* Gervais and Verreaux, 1842, CM 11899.

The shape of the element of Paaw reported for *Philander opossum*, CM 110578, was essentially repeated in the rest

of the CM *Philander opossum* sample preserving the bone. Contact between the element of Paaw and the pars cochlearis as in CM 110578 occurred in about three-quarters of the *Philander opossum* sample; when there was no contact, the two bones were close.

In the remaining CM marsupials, the shape of the element of Paaw was a uniform straight rod (*Gracilianus*, *Lutreolina*, *Marmosa*, *Marmosops*, *Thylamys*, *Antechinus*, *Dasyuroides*, *Dasyurus*, *Perameles*, and *Vombatus*), a straight rod strongly tapered anteriorly (*Caluromys*, *Didelphis*, *Metachirus*, and *Monodelphis*), and a curved element wider posteriorly as in *Philander opossum* (*Chironectes*). It was only in didelphids that there was contact between the element of Paaw and the pars cochlearis, but as with *Philander opossum*, such contact was not present in all specimens.

DISCUSSION

The Element of Paaw in Marsupials

Our review of the literature, the collections of Carnegie Museum of Natural History, and online specimens at Digimorph.org and MorphoSource.org shows that an element of Paaw is present in representatives of all seven orders of extant marsupials (Tables 3–5). Moreover, we found the element of Paaw to be a substantial structure, longer than the stapedial footplate, in representatives of four orders: Didelphimorphia, Microbiotheria, Peramelemorphia, and Notoryctemorphia, whereas it is shorter than the footplate in Paucituberculata. We were not able to accurately measure the element in Dasyuromorphia and Diprotodontia, but our impression is that it is at least as long as the stapedial footplate. In Didelphimorphia, the most diverse order in the CM collections, we found the element in all 11 represented genera (Table 5), out of the 18 reported by Burgin et al. (2018). In total, we found the element of Paaw in 41 marsupial species (Tables 3–5), out of the 379 reported by Burgin et al. (2018).

The CM sample included 27 marsupial species with the element of Paaw (Table 5) and 17 in which the element was absent or could not be confirmed (Table 6). Of the 27 species with the element, 15 had 100% bilateral occurrence; the remainder had some mix of bilateral and unilateral occurrence and four of these had some specimens with no element of Paaw. Our illustrations of the left and right elements in *Philander opossum*, CM 110578 (Fig. 11G–J) reveal some asymmetry, which we also noted in other CM marsupials but did not record. Intraspecific variation in the presence/absence of the element of Paaw has been reported for some bats (Hinchcliffe and Pye 1969) and armadillos (Basso et al. 2020), and presence on one side only has been reported in the treeshrew *Tupaia* (Hinchcliffe and Pye 1969) and the large hairy armadillo *Chaetophractus villosus* (Desmarest, 1804) (Basso et al. 2020). However, note that in the two studies reporting variation (Hinchcliffe and Pye 1969; Basso et al. 2020), the specimens examined began as whole heads that were either serially sectioned or CT scanned and were not museum osteological specimens. The variable incidence of the element of Paaw in some species of CM marsupials may be true variation, but it may also result from preparation techniques used to produce museum specimen, a view that we favor. The absence of the element of Paaw in CM marsupials was noted most frequently in specimens that also lacked auditory ossicles. There is little that holds the element of Paaw in place beyond its soft tissue connection to the stapes, the pars cochlearis, and the stapedius fossa. With the usual removal of soft tissue in museum specimen preparation, it is not surprising that we encountered the element of Paaw missing as well. The only way to truly evaluate the incidence of this structure is through head dissection or serial section, either with a microtome or with an x-ray beam, as done by Hinchcliffe and Pye (1969) and Basso et al. (2020), respectively.

Other variables regarding the element of Paaw in the studied sample are its size and shape and its contact with the pars cochlearis. The general pattern is to have the anterior part of the element in contact with or very close to the pars cochlearis, with connective tissue cementing the relationship. There are clear exceptions where the element is widely separated from possible petrosal contact (e.g., *Notoryctes typhlops*, UMZC A5. 1/1). A concern that cannot be overlooked regarding the presence or absence of contact is the effect of drying and shrinkage that occurs in museum specimen preparation on the position of the element of Paaw. We hypothesize that the petrosal contact is real in light of the frequency of connective tissue attachment, but further studies on wet specimens, either through dissection, serial sectioning, or CT scanning, are needed to address this.

Based on the distribution of the element of Paaw across all extant marsupial orders, we hypothesize its presence to be primitive for Marsupialia. We are less certain about the presence or absence of the element at the level of Placentalia or Theria. The element's currently known distribution across Placentalia is patchy (Table 2), although it occurs in representatives of three of the four higher-level placental clades (in Xenarthra, Euarchontoglires, and Laurasiatheria, but unreported in Afrotheria). A caveat here is that a study like ours for marsupials with museum osteological specimens and primary CT scan data has not been done for a broad spectrum of placentals, aside from our study of the 169 coronal CT slice movies available on DigiMorph.org. Until that is accomplished, the ancestral condition of the element of Paaw for Placentalia and Theria is best considered uncertain. Additionally, to date, an element of Paaw has not been reported for any fossil mammal, although this is not surprising, given the element's loose attachment to the basicranium. There are possible exceptions to this: long muscular processes of the stapes have been described for the Middle Jurassic haramiyidan *Arboroharamiya jenkinsi* Zheng et al., 2013 (Meng et al. 2018) and the Early Cretaceous eutriconodontan *Chaoyangodens lii* Hou and

TABLE 3. Incidences of element of Paaw in coronal slice movies on DigiMorph.org at the University of Texas at Austin (see Appendix 1).

Order	Family	Species	Specimen #	Age	Slice #
Didelphimorphia	Didelphidae	*Chironectes minimus*	AMNH 129701	adult	1345
Didelphimorphia	Didelphidae	*Monodelphis domestica*	TTM M-7595	day 27	411
Didelphimorphia	Didelphidae	*Monodelphis domestica*	TTM M-7536	day 48	316
Didelphimorphia	Didelphidae	*Monodelphis domestica*	TTM M-8266	day 56	687
Didelphimorphia	Didelphidae	*Monodelphis domestica*	TTM M-7539	day 57	335
Didelphimorphia	Didelphidae	*Monodelphis domestica*	TTM M-7542	day 75	417
Didelphimorphia	Didelphidae	*Monodelphis domestica*	TTM M-7545	day 90	403
Didelphimorphia	Didelphidae	*Monodelphis domestica*	TTM M-7599	adult	403
Paucituberculata	Caenolestidae	*Caenolestes fulginosus*	KU 124015	adult	799
Microbiotheria	Microbiotheriidae	*Dromiciops gliroides*	FMNH 127463	adult	589
Dasyuromorphia	Dasyuridae	*Sminthopsis crassicaudata*	AMNH 126686	adult	580
Peramelemorphia	Perameledae	*Echymipera kalubu*[1]	AMNH 190970	adult	429
Peramelemorphia	Thylacomyidae	*Macrotis lagostis*	AMNH 74486	adult	468
Diprotodontia	Burramyidae	*Cercartetus caudatus*	AMNH 155090	adult	571
Diprotodontia	Pseudocheiridae	*Petauroides volans*[1]	AMNH 15005	adult	534
Cingulata	Dasypodidae	*Dasypus novemcinctus*[2]	TTM M-7147	adult	603

[1]Element of Paaw on right side only.
[2]*Dasypus novemcinctus,* TMM M-7147, Dr. Ted Macrini, 2005, "Dasypus novemcinctus" (On-line), Digital Morphology. Accessed April 8, 2021 at http://digimorph.org/specimens/Dasypus_novemcinctus/

Meng, 2014 (Meng and Hou 2016), with that in the former longer than the stapedial footplate length. These long muscular processes may represent an element of Paaw fused to the stapes (as suggested in Fig. 1F). New discoveries of Mesozoic mammals may resolve the homologies of these structures.

Regarding the function of the element of Paaw, three primary functions are attributed to the stapedius and tensor tympani muscles (Pilz et al. 1997:180). "First, they prevent desensitization, i.e., overloading of the sensory receptors of the cochlea, thereby maintaining a good level of sensitivity… Second, in mammals it is well established that the action of the middle ear muscles decreases mainly lower frequencies… Third, the middle ear muscles protect the ear from noise damage… The three functions of the middle ear muscles are incorporated in the desensitization, interference and injury-preventing theory (DIIP) by Borg et al. (1984)." Some authors (e.g., McCrady 1938; McClain 1939; Henson 1961) have considered the element of Paaw to function as a sesamoid bone, whereas others (e.g., Sánchez-Villagra et al. 2002) disagree with the sesamoid analogy. One's view on this really depends on one's definition of a sesamoid bone. In a recent review paper on sesamoids in tetrapods, Abdala et al. (2019: 2) noted "Sesamoids are currently defined as any organized intratendinous/intraligamentous structure, including those composed by fibrocartilage, adjacent to an articulation or joint." By this broad definition, the element of Paaw with its tip within the tendon of the stapedius muscle near the stapes is a sesamoid bone. Sesamoids are generally held to serve a mechanical role: the patella, for example, acts as a fulcrum, increasing the lever arm of the quadriceps, but does so by pivoting against the femur (Fox et al. 2012). Mechanical roles have been suggested for the element of Paaw: reduction of friction between the stapedius tendon and the enveloping middle ear mucosa (Henson 1961; Hinchcliffe and Pye 1969) or "concentrating and transmitting forces between the stapedial muscle and the stapes"

TABLE 4. Measurements of the element of Paaw and stapedial footplate from CT scanned marsupials, all downloaded from MorphoSource.org, with the exception of *Philander opossum* (this study).

Order	Species	Specimen #	Skull length	Elem. Paaw length	Elem. Paaw width	Elem. Paaw surface area	Elem. Paaw volume	Stapes foot-plate length	Stapes foot-plate width	Stap. ratio (l/w)
Didelphimorphia	*Caluromys* sp.[1]	DU EA 162	60.45	1.05	0.18	0.478	0.014	0.65	0.35	1.86
	Caluromysiops irrupta[1]	FMNH 60698	74.70	0.93	0.46	0.908	0.054	0.87	0.42	2.07
	Didelphis marsupialis[1]	DU BAA 0164	55.69	0.64	0.27	0.803	0.071	0.42	0.27	1.56
	Didelphis sp.[2]	DU EA 202	84.30	0.71	0.33	0.737	0.045	0.50	0.33	1.52
	Monodelphis domestica[2]	AMNH 261241	35.72	0.61	0.24	0.362	0.013	0.47	0.28	1.68
	Philander opossum[1]	CM 110578	75.62	1.32	0.50	1.165	0.062	0.62	0.41	1.48
Paucituberculata	*Rhyncholestes raphanurus*[2]	FMNH 127476	31.62	0.28	0.15	0.092	0.002	0.40	0.28	1.42
Microbiotheria	*Dromiciops gliroides*[2]	UMMZ 156354	28.84	0.57	0.20	0.265	0.007	0.48	0.25	1.92
Peramelemorphia	*Isoodon obesulus*[2]	UMZC A7. 4/5	70.05	0.72	0.33	0.654	0.036	0.61	0.37	1.65
Notoryctemorphia	*Notoryctes typhlops*[2]	UMZC A5. 1/1	25.36	0.92	0.35	0.671	0.021	0.80	0.57	1.40

[1]Measurements based on left side.
[2]Measurements based on right side.

(Sánchez-Villagra et al. 2002: 234). However, in the most recent pronouncement on function of the element of Paaw, Basso et al. (2020:12) stated "The intra-specific variability that has been documented previously (Hinchcliffe & Pye, 1969) and was also found in the present study suggests that the element of Paaw has no vital function." This may be true for the small elements of Paaw reported in some armadillos by Basso et al. (2020), but it is hard to imagine that a structure with a larger volume than the stapes (as in *Philander opossum*, CM 110578) that we surmise is universally present in a number of related taxa does not have a vital function. Given that we found the element of Paaw in *Philander opossum*, CM 110578, to be in broad contact with the pars cochlearis posterior to the fenestra vestibuli (Figs. 5B, 12B, C) and observed similar contact in the vast majority of the marsupial specimens examined, we suggest the element of Paaw acts as a sesamoid bone in most marsupials, increasing the lever arm of the stapedius muscle.

Mammals are not the only tetrapods with sesamoid bones in the head. The review paper by Abdala et al. (2019) presented seven examples that have been reported from non-mammalian tetrapods. Only one of these bears any similarity positionally to the mammalian element of Paaw, the sesamoid in the squamosal-columellar ligament in some salamanders. Although it has an attachment to the homologous bone (columella=stapes), it is not associated with muscle.

The Stapedial Ratio

The stapedial ratio was introduced by Segall (1970: 170–171), who noted "Since the stapes plate, with the help of the stapedial ligaments, fits snugly into the fenestra ovalis [vestibuli], the contours of the latter give an exact outline of the plate. Therefore, measurements of the fenestra were taken in specimens lacking the stapes…Measurements of the fenestra ovalis were easier to take and for this reason proved even more exact than the measurements of the stapes ratio based on the stapes in place. The results were repeatedly checked, and small differences were often found. The figures arrived at are, therefore, meaningful approximations." Segall (1970) reported the stapedial ratio to be 1.0 (i.e., round) in the monotreme *Tachyglossus* Illiger, 1811, between 1.1 and 2.1 in a sample of marsupials, and between 1.8 and 2.9 in a sample of placentals. Rounded as primitive for mammals, as suggested by Segall (1970), has been supported by subsequent studies of Mesozoic mammaliaforms (Wible and Hopson 1993). Of the 18 genera of marsupials examined by Segall (1970), five are in our study (*Caluromys* J.A. Allen, 1900, *Didelphis*, *Philander*, *Dromiciops* Thomas, 1894, and *Notoryctes* Stirling, 1891, in Table 4). The ratios are the same in *Notoryctes* (1.4) and comparable in *Philander* (1.5 vs. ours at 1.48), and less so in *Didelphis* (1.3 vs. ours at 1.52 and 1.56), *Dromiciops* (2.1 vs. ours at 1.92), and *Caluromys* (1.5 vs. ours at 1.86). Segall (1970) did not include species or specimen numbers.

Horovitz et al. (2008) examined the dimensions of the fe-

TABLE 5. Incidence of element of Paaw in CM marsupial specimens.

Order	Species	Number of specimens examined	Number (%) with two elements of Paauw	Number (%) with one element of Paauw	Number (%) with no element of Paaw	Examples with element of Paaw
Didelphimorphia	*Caluromys derbianus*	2	0 (0%)	1 (50%)	1 (50%)	CM 51988
	Caluromys philander	3	0 (0%)	3 (100%)	0 (0%)	CM 4680, 52689, 52690
	Chironectes minimus	2	2 (100%)	0 (0%)	0 (0%)	CM 98580, 119053
	Didelphis albiventris	15	13 (87%)	0 (0%)	2 (13%)	CM 42774, 80013
	Didelphis marsupialis	59	43 (73%)	9 (15%)	7 (12%)	CM 52707, 52712
	Didelphis virginiana	100	36 (36%)	25 (25%)	39 (39%)	CM 23802, 33648
	Gracilinanus agilis	3	2 (67%)	1 (33%)	0 (0%)	CM 1854, 2168, 80015
	Gracilinanus dryas	1	1 (100%)	0 (0%)	0 (0%)	CM 70720
	Lutreolina crassicaudata	3	2 (67%)	0 (0%)	1 (33%)	CM 42775, 42778
	Marmosa demerarae	5	5 (100%)	0 (0%)	0 (0%)	CM 63503, 63504
	Marmosa mexicana	94	91 (97%)	3 (3%)	0 (0%)	CM 112874, 112875
	Marmosa murina	17	16 (94%)	1 (6%)	0 (0%)	CM 68349
	Marmosa rapposa	6	6 (100%	0 (0%)	0 (0%)	CM 2754, 5049
	Marmosa robinsoni	10	9 (90%)	1 (10%)	0 (0%)	CM 1015
	Marmosops dorothea	1	1 (100%)	0 (0%)	0 (0%)	CM 4979
	Metachirus nudicaudatus	3	3 (100%)	0 (0%)	0 (0%)	CM 12173, 52728, 78215
	Monodelphis arlindoi	7	5 (71%)	2 (29%)	0 (0%)	CM 68358, 68359
	Monodelphis brevicaudata	2	2 (100%)	0 (0%)	0 (0%)	CM 52730, 68360
	Monodelphis dimidiata	2	1 (50%)	1 (50%)	0 (0)%	CM 86609
	Monodelphis domestica	26	26 (100%)	0 (0%)	0 (0%)	CM 80017, 80025
	Monodelphis glirina	2	2 (100%)	0 (0%)	0 (0%)	CM 4681, 5061
	Monodelphis osgoodi	1	0 (0%)	1 (100%)	0 (0%)	CM 5242
	Monodelphis touan	4	4 (100%)	0 (0%)	0 (0%)	CM 76731, 76730
	Philander opossum	58	56 (95%)	0 (0%)	2 (5%)	CM 61833, 76748, 110578
	Thylamys cinderella	18	4 (22%)	14 (78%)	0 (0%)	CM 42784, 42787
	Thylamys pusillus	3	2 (67%	1 (33%)	0 (0%)	CM 42800, 42803
	Thylamys venustus	2	0 (0%)	2 (100%)	0 (0%)	CM 5227, 5231
Dasyuromorphia	*Antechinus stuartii*	16	16 (100%)	0 (0%)	0 (0%)	CM 50824, 50825
	Dasyuroides byrnei	2	2 (100%)	0 (0%)	0 (0%)	CM 50840, 50841
	Dasyurus maculatus	1	1 (100%)	0 (0%)	0 (0%)	CM 50842
Peramelemorphia	*Perameles nasuta*	1	1 (100%)	0 (0%)	0 (0%)	CM 20977
Diprotodontia	*Vombatus ursinus*	1	1 (100%)	0 (0%)	0 (0%)	CM 50801

nestra vestibuli in a larger number of marsupials, including multiple specimens for ten didelphid species. They found intraspecific variation as well as left/right asymmetry in the stapedial ratios. For *Philander opossum*, for example, they reported on 13 oval windows, with a low ratio of 1.23 and high of 1.88, and a mean of 1.46 (close to CM 110578 at 1.48). There were two specimens of *Philander opossum* with the left and right sides measured, with values of 1.42 vs. 1.64 and 1.44 and 1.36, respectively. The other two species in common between Horovitz et al. (2008) and our study (Table 4) are *Monodelphis domestica* (1.26 and 1.46 vs. 1.68) and *Notoryctes typhlops* (1.57 vs. 1.40).

Ekdale (2011) reported considerable variation in the fenestra vestibuli in a sample of 65 isolated petrosals of Pleistocene elephantimorphs from Friesenhahn Cave in Texas. The ratio of fenestra length to width ranged from 1.4 to 2.1 with a mean of 1.8. It is unclear how many taxa are represented in this sample, although 97 percent of the teeth from the cave are *Mammuthus* Brookes, 1828, with the remainder *Mammut* Blumenbach, 1799. For one specimen, Ekdale (2011) calculated the ratio based on both the fenestra vestibuli and the stapedial footplate and found the former to be slightly larger than the latter (1.8 vs. 1.7). Discrepancy in the dimensions of the fenestra vestibuli and stapedial footplate has been reported in other placentals (e.g., *Spalax* Güldenstaedt, 1770, Mason et al. 2010; *Gerbillurus setzeri* Schlitter, 1973, Mason 2016; *Heterocephalus glaber* Rüppell, 1842, Mason et al. 2016). These observations contradict Segall's (1970) insistence that the ratios based on these structures correspond.

A character of the stapedial ratio is frequently used in phylogenetic analyses, with states equal to or below 1.8 or above 1.8, which is said to capture rounded versus elliptical (e.g., Bi et al. 2018). The discrepancies between ratios based on the stapedial footplate versus the fenestra vestibuli in the same specimen reported by Ekdale (2011), the discrepancies in the size of the footplate and fenestra in some rodents (Mason et al. 2010, 2016; Mason 2016), and the range of intraspecific variation and left/right asymmetry reported by Horovitz et al. (2008) represent cautionary tales regarding the use of this character. Nevertheless, despite the range of intraspecific variation in the didelphids studied by Horovitz et al. (2008), only one, *Philander opossum*, would be scored as polymorphic for this character and that based on a single specimen above 1.8 (at 1.88). A more fundamental concern is the significance of the cut-off of 1.8. When a larger comparative dataset is available, this character should be reviewed for alternative partitioning of states.

SUMMARY

(1) The osseous structures of the middle ear of the didelphimorphian *Philander opossum* are described in detail based on CT scans of CM 110578. Certain osteological features are sampled in an additional 57 *Philander opossum* specimens in the CM collection. Fifty-six of 58 specimens have a substantial ossified element of Paaw, and in three-quarters of these, the element contacts the petrosal behind the fenestra vestibuli. We suggest that the absence of the element in two specimens and the absence of petrosal contact for the element in one quarter of the sample result from the preparation process and are not true variation. We further suggest that because of its contact with the petrosal, the element of Paaw functions as a sesamoid bone, increasing the lever arm of the stapedius muscle.

(2) We sampled 386 specimens from 26 additional didelphimorphian species in the CM collection and encountered results for the element of Paaw like those for *Philander opossum*. Ten species have 100% bilateral occurrence of an ossified element, whereas the remainder have a mix of bilateral and unilateral occurrence and absence. There is also a mix of specimens with and without petrosal contact for the element. As hypothesized for *Philander opossum*, we suggest that these differences result from the preparation process and are not true variation. We also propose that the element of Paaw functions as a sesamoid bone in didelphimorphians. A difference across the didelphimorphian sample is the shape of the element of Paaw, which ranges between a uniform straight rod, a straight rod tapering anteriorly, and a bent triangular shape.

(3) The sample sizes for non-didelphimorphian marsupials available in the CM collections, DigiMorph.org, and MorphoSource.org are much smaller. Along with our observations on Didelphimorphia, we report an ossified element of Paaw in some representatives of the remaining extant marsupial orders: Paucituberculata, Microbiotheria, Dasyuromorphia, Notoryctemorphia, Peramelemorphia, and Diprotodontia, supporting the presence of the element in the marsupial common ancestor. The element in most specimens is a uniform straight rod with petrosal contact, suggesting a sesamoid function. However, there are clear instances (e.g., *Notoryctes typhlops*) where the element has no petrosal contact, suggesting the sesamoid analogy is not ubiquitous in Marsupialia.

(4) We compare the petrosals in the didelphimorphians *Philander opossum*, *Didelphis marsupialis*, and *Monodelphis domestica*. Major differences concern features associated with the course of certain veins and nerves. *Philander* and *Didelphis* have a foramen for the prootic sinus formed by the petrosal, which has not been reported previously for these taxa; the foramen is lacking in *Monodelphis*. *Philander* and *Didelphis* also have a well-developed posttemporal groove, which is essentially absent in *Monodelphis*. There is a difference in the extent of the floor of the cavum supracochleare, which impacts the relationship between the secondary facial foramen and the foramen for the prootic canal. These foramina have a common aperture in *Didelphis*, are connected by a ridge in *Philander*, and are fully separated in *Monodelphis*.

(5) We calculate the stapedial ratio (length/width of the stapedial footplate) for ten marsupials based on CT scans. Our results add to a growing literature that raises questions about the utility of this ratio and a similar ratio of the length/width of the fenestra vestibuli in phylogenetic analyses. Concerns are intraspecific variation and the discrepancy between the dimensions of the footplate on the one hand and the oval window on the other.

ACKNOWLEDGMENTS

We thank the organizers of MorphoSource.org and DigiMorph.org for their foresight in creating online repositories for CT scanned data. Without access to these data, our study would not have been possible. We thank Paul Bowden for producing Figure 1. We are grateful to Mathew

J. Mason and Marcelo R. Sánchez-Villagra for their insightful reviews that greatly improved our final paper. Funding for this project is from National Science Foundation Grant DEB 1654949, the Carnegie Museum of Natural History, and the R.K. Mellon North American Mammal Research Institute.

LITERATURE CITED

ABDALA, V., M.C. VERA, L.I. AMADOR, G. FONTANARROSA, J. FRATANI, AND M.L. PONSSA. 2019. Sesamoids in tetrapods: the origin of new skeletal morphologies. Biological Reviews, 94(6):2011–2032.

ALLEN, J.A. 1900. Note on the generic name *Didelphis* and *Philander.* Bulletin of the American Museum of Natural History, 13(15):185–190.

ALLIN, E.F., AND J.A. HOPSON. 1992. Evolution of the auditory system in Synapsida ("mammal-like reptiles" and primitive mammals) as seen in the fossil record. Pp. 587–614, *in* The Evolutionary Biology of Hearing (D.B. Webster, A.N. Popper, and R.R. Fay, eds.). Springer-Verlag, New York.

ARCHER, M. 1976. The basicranial region of marsupicarnivores (Marsupialia), interrelationships of carnivorous marsupials, and affinities of the insectivorous peramelids. Zoological Journal of the Linnean Society, 59:217–322.

ASHERSON, N. 1978. The fourth auditory ossicle: fact or fantasy? The Journal of Otology and Laryngology, 92:453–465.

BASSO, A.P., N.S. SIDORKEWICJ, E.B. CASANAVE, AND M.J. MASON. 2020. The middle ear of the pink fairy armadillo *Chlamyphorus truncatus* (Xenarthra, Cingulata, Chlamyphoridae): comparison with armadillo relatives using computed tomography. Journal of Anatomy. doi: 10.1111/joa.13146.

BI, S., X. ZHENG, X. WANG, N. CIGNETTI, S. YANG, AND J.R. WIBLE. 2018. An Early Cretaceous eutherian and the placental-marsupial dichotomy. Nature, 558:390–395.

BLUMENBACH, J.F. 1799. Handbuch der Naturgeschichte. Vol. 6. J.C. Dieterich, Göttingen.

BONDY, G. 1907. Beiträge zur vergleichenden Anatomie des Gehörorgans der Säuger. (Tympanicum, Membrana Shrapnelli und Chordaverlauf). Anatomische Hefte, 35:293–408.

BORG, E., S.A. COUNTER, AND G. RÖSLER. 1984. Theories of middle-ear muscle function. Pp. 63–99, *in* The Acoustic Reflex (S. Silman, ed.). Academic Press, Orlando.

BRISSON, M.J. 1762. Le regnum animale in classes IX distributum, sive synopsis metodica sistens generalem animalium distribution in classes IX, and duarum primarium classium, quadrupedum scilicet and cetaceorum, particularem dibvisionem in ordines, sectiones, genera and species. T. Haak, Paris.

BROOKES, J. 1828. A Catalogue of the Anatomical and Zoological Museum of Jeshua Brookes, Esq., F.R.S. etc. Part 1. R. Taylor, London. 76 pp.

BURFORD, C.M., AND M.J. MASON. 2016. Early development of the malleus and incus in humans. The Anatomical Record, 228:857–870.

BURGIN, C.J., J.P. COLELLA, P.L. KAHN, AND N.S. UPHAM. 2018. How many species of mammals are there? Journal of Mammalogy, 99(1):1–14.

BURNETT, G.T. 1830. Illustrations of the Quadrupedia, or quadrupeds, being the arrangement of the true four-footed beasts. Quarterly Journal of Literature, Science and the Arts, July to December, 1829:336–353.

CABEZUDO, L., F. ANTOLI-CANDELA, JR., AND J. SLOCKER. 1983. Morphological study of the middle and inner ear of the bat: *Myotis myotis*. Advances in Oto-Rhino-Laryngology, 31:28–38.

CARMINO, M.Á.-B., AND M.Á.-B. BLANCO. 2018. Stapedius tendon ossification: meaning of the ossicle of Paaw. Revista Portuguesa de Otorrinolaringologia e Cirurgia de Cabeça e Pescoço, 56(1):35–37.

CHAUVEAU, A. 1871. Traité d'anatomie comparée des animaux domestique. Second edition. J.-B. Baillière, Paris.

CLARK, C.T., AND K.K. SMITH. 1993. Cranial osteogenesis in *Monodelphis domestica* (Didelphidae) and *Macropus eugenii* (Macropodidae). Journal of Morphology, 215:119–149.

COLLETT, R. 1884. On some apparently new marsupials from Queensland. Proceedings of the Zoology Society of London, XXVI:381–388, pls. 29–32.

———. 1895. On a new *Pseudochirus* from northwest Australia. Zoologischer Anzeiger, 18(490):464–468.

COUES, E. 1872. On the osteology and myology of *Didelphys virginiana.* Memoirs read before the Boston Society of Natural History, 2:41–149.

DESMAREST, A.G. 1804. Tableau méthodique des mammifères. Pp. 5–58, *in* Nouveau dictionnaire d'histoire naturelle, Vol. 24. Chez Deterville, Paris.

———. 1822. Mammalogie, ou description des espèces de mammifères. Seconde Partie, contenant les orders des bimanes, des quadrumanes et des carnassiers. V. Agasse, Paris.

DOM, R., B.L. FISHER, AND G.F. MARTIN. 1970. The venous system of the head and neck of the opossum (*Didelphis virginiana*). Journal of Morphology, 132:487–496.

DORAN A.H.G. 1878. Morphology of mammalian ossicula auditûs. Transactions of the Linnean Society of London, second series, Zoology, 1:391–497.

EKDALE, E.G. 2011. Morphological variation in the ear region of Pleistocene Elephantimorpha (Mammalia, Proboscidea) from central Texas. Journal of Morphology, 272(4):452–464.

———. 2013. Comparative anatomy of the bony labyrinth (inner ear) of placental mammals. PLoS ONE, 8(6):e66624.

EVANS, H.E. 1993. Miller's Anatomy of the Dog. W.B. Saunders, Philadelphia. 1113 pp.

FILAN, S.L. 1991. Development of the middle ear region in *Monodelphis domestica* (Marsupialia, Didelphidae): marsupial solutions to an early birth. Journal of Zoology, 225:577–588.

FISCHER, J.B. 1829. Synopsis mammalium. Sumtibus J.C. Cottae, Stuttgardtiae.

FLEISCHER, G. 1973. Studien am Skelett des Gehörorgans der Säugetiere, einschließlich des Menschen. Säugetierkundliche Mitteilungen, 21:131–239.

———. 1978. Evolutionary principles of the mammalian middle ear. Advances in Anatomy, Embryology and Cell Biology, 55:1–70.

FOX, A.J.S., F. WANIVENHAUS, AND S.A. RODEO. 2012. The basic science of the patella: structure, composition, and function. Journal of Knee Surgery, 25:127–142.

GERVAIS, M.P., AND M.J. VERREAUX. 1842. On a new genus of marsupial animals, *Tarsipes rostratus*. Proceedings of the Zoological Society of London, 1842(10):1–5.

GOLDFUSS, G.A. 1817. *In* Die Säugethiere (J.C.D. von Schreber, ed.). Abbildungen nach der Natur, mit Beschreibungen. Fortgesetzt von A. Goldfuss, 65e cahier.

GOULD, J. 1842. Characters of a new species of *Perameles*, and a new species of *Dasyurus*. Proceedings of the Zoological Society of London, 1841(10):41–42.

———. 1844. Exhibition and character of a number of animals, &c. transmitted from Australia by Mr. Gilbert. Proceedings of the Zoological Society of London, 1844(12):103–107.

GRABOYES, E.M., R.A. CHOLE, AND T.E. HULLAR. 2011a. The ossicle of Paaw. Otology & Neurotology, 32:1185–1188.

GRABOYES, E.M., T.E. HULLAR, AND R.A. CHOLE. 2011b. The lenticular process of the incus. Otology & Neurotology, 32:1600–1604.

GRAY, J.E. 1858. A list of species of Mammalia sent from the Aru Islands by Mr. A.R. Wallace to the British Museum. Proceedings of the Zoological Society of London, 1858(26):106–114.

GÜLDENSTAEDT, A. 1770. *Spalax*, novum glirium genus. Novi Commentarii Academiae Petropolitanae, 14:409–440.

HAN, G., F. MAO, S. BI, Y. WANG, AND J. MENG. 2017. A Jurassic gliding euharamiyidan mammal with an ear of five auditory bones. Nature, 551(7681):451–456.

HARRIS, G.P. 1808. Description of two new species of *Didelphis* from Van Diemen's Land. Transactions of the Linnean Society of London, 9:174–178.

HENSON, O.W., JR. 1961. Some morphological and functional aspects of

certain structures of the middle ear in bats and insectivores. Kansas University Science Bulletin, 41:151–255.

———. 1974. Comparative anatomy of the middle ear. Pp. 39-110, *in* Handbook of Sensory Physiology. Volume V/1. Auditory System: Anatomy, Physiology (Ear) (W.D. Keidel and W.D. Neff, eds.). Springer-Verlag, Berlin Heidelberg New York.

HINCHCLIFFE, R., AND A. PYE. 1969. Variations in the middle ear of the Mammalia. Journal of Zoology, 157:277–288.

HOROVITZ, I., S. LADEVÈZE, C. ARGOT, T.E. MACRINI, T. MARTIN, J.J. HOOKER, C. KURZ, C. DE MUIZON, AND M.R. SÁNCHEZ-VILLAGRA. 2008. The anatomy of *Herpetotherium* cf. *fugax* Cope, 1873, a metatherian from the Oligocene of North America. Palaeontographica Abteilung A, 284:109–141.

HOU, S.-L., AND J. MENG. 2014. A new eutriconodont mammal from the Early Cretaceous Jehol Biota of Liaoning, China. Chinese Science Bulletin, 59**:**546–553.

HYRTL, J. 1845. Vergleichend-anatomische Untersuchungen über das innere Gehörorgan des Menschen und der Säugethiere. Verlag von Friedrich Ehrlich, Prag. 139 pp. + 9 plates.

———. 1850. Zur vergleichenden Anatomie der Trommelhöhle. Denkschriften der kaiserlichen Akademie der wissenschaften/mathematisch-naturwissenschaftliche Classe Wien, 1:29–37 + 6 figures.

ILLIGER, J.K.W. 1811. Prodromus Systematis Mammalium et Avium additis terminis zoographicis untriusque classis, eorumque versione Germanica. Sumptibus C. Salfield, Berlin.

JACKSON, C.M. (ED.). 1914. Morris's Human Anatomy, 5th edition. P. Blakiston's Son & Co., Philadelphia. 1539 pp.

JANSA, S.A., F.K. BARKER, AND R.S. VOSS. 2014. The early diversification history of didelphid marsupials: a window into South America's "splendid isolation." Evolution, 68(3):684–695.

KAMPEN, P.N. VAN. 1905. Die Tympanalgegend des Säugetierschädels. Gegenbaurs Morphologisches Jahrbuch, 34:321–722.

KERR, R. 1792. The Animal Kingdom, or Zoological System, of the Celebrated Sir Charles Linnaeus. Class I. Mammalia. London. 651 pp.

KLAAUW, C.J. VAN DER. 1923. Die Skelettstückchen in der Sehne des Musculus stapedius und nahe dem Ursprung der Chorda tympani. Zeitschrift für Anatomie und Entwicklungsgeschicte, 69:32–83.

———. 1931. The auditory bulla in some fossil mammals with a general introduction to this region of the skull. Bulletin of the American Museum of Natural History, 62(1):1–352.

KOPSCH, F. (ED.). 1909. Rauber's Lehrbuch der Anatomie des Menschen, Abteilung 6: Sinnesorgane und General-Register, 8th edition. Georg Thieme, Leipzig. 314 pp.

KUROSAKI, Y., K. KUROMOTO, K. MATSUMOTO, Y. ITAI, A. HARA, AND J. KUSAKARI. 1995. Congenital ossification of the stapedius tendon: diagnosis with CT. Radiology, 195:711–714.

LINNAEUS, C. 1758. Systema Naturae per regna tria naturae, secundum classis, ordines, genera, species cum characteribus, differentiis, synonymis, locis. Editio Decima, Reformata. Tomus I. Laurentii Salvii, Stockholm. 824 pp.

MACPHEE, R.D.E. 1981. Auditory regions of primates and eutherian insectivores: morphology, ontogeny, and character analysis. Contributions to Primatology, 18:1–282.

MAIER, W. 1987. Der Processus angularis bei *Monodelphis domestica* (Didelphidae; Marsupialia) und seine Beziehungen zum Mittelohr: Eine ontogenetische und evolutionsmorphologie Untersuchung. Gegenbaurs Morphologisches Jahrbuch, 133**:**123–161.

MAO, F., C. LIU, M.H. CHASE, A.K. SMITH, AND J. MENG. 2020. Exploring ancestral phenotypes and evolutionary development of the mammalian middle ear based on Early Cretaceous Jehol mammals. National Science Review, nwaa188. https://doi.org/10.1093/nsr/nwaa188.

MASON, M.J. 2016. Structure and function of the mammalian middle ear. I: large middle ears in small desert mammals. Journal of Anatomy, 228:284–299.

MASON, M.J., H.L. CORNWALL, AND E.S.J. SMITH. 2016. Ear structures of the naked mole-rat, *Heterocephalus glaber*, and its relatives (Rodentia: Bathyergidae). PLoS ONE, 11(12):e0167079.

MASON, M.J., F.W.S. LAI, J.-G. LI, AND E. NEVO. 2010. Middle ear structure and bone conduction in *Spalax*, *Eospalax*, and *Tachyoryctes* mole-rats (Rodentia: Spalacidae). Journal of Morphology, 271:462–472.

MCCLAIN, J.A. 1939. The development of the auditory ossicles of the opossum (*Didelphys virgininia*). Journal of Morphology, 64:211–250.

MCCRADY, E. 1938. The Embryology of the Opossum. Memoirs of the Wistar Institution, Philadelphia.

MENG, J., S. BI, X. ZHENG, AND X. WANG. 2018. Ear ossicle morphology of the Jurassic euharamiyidan *Arboroharamiya* and evolution of mammalian middle ear. Journal of Morphology, 279(4):441–457.

MENG, J., AND S.-L. HOU. 2016. Earliest known mammalian stapes from an Early Cretaceous eutriconodontan mammal and implications for transformation of mammalian middle ear. Palaeontologia Polonica, 67:181–196.

MENG, J., F. MAO, G. HAN, X.-T. ZHENG, X.-L. WANG, AND Y. WANG. 2020. A comparative study on auditory and hyoid bones of Jurassic euharamiyidans and contrasting evidence for mammalian middle ear evolution. Journal of Anatomy, 236(1):50–71.

MILNE-EDWARDS, A. 1877. Note sur quelques mammiferes nouveaux provenant de la Nouvelle-Guinee. Comptes Rendu Hebdomodaires des Séances de l'Académie des Sciences, 85:1079–1081.

NAPIER, J.R., AND P.H. NAPIER. 1967. A Handbook of Living Primates. Academic Press, New York. 456 pp.

NOMINA ANATOMICA VETERINARIA, 6th Edition. 2017. Editorial Committee, Hannover, Ghent, Columbia, Rio de Janeiro. http://www.wava-amav.org/wava-documents.html

OSGOOD, W.H. 1924. Review of living caenolestids with description of a new genus from Chile. Field Museum of Natural History Publication, Zoological Series, 14: 165–173.

Owen, R. 1838. *In* Three Expeditions into the Interior of Eastern Australia, with Descriptions of the Recently Explored Region of Australia Felix and of the Present Colony of New South Wales (Mitchell, T.L., ed.). Mitchell, T & W. Boone, London.

PALLAS, P.S. 1766. Miscellanea zoologica, quibus novae imprimis atque obscurae animalium species describuntur et obsevationibus iconibusque illustrantur. Van Cleef, Den Haag. 224 pp.

PARKER, W.K. 1874. On the structure and development of the skull in the pig (*Sus scrofa*). Philosophical Transactions of the Royal Society of London, 164:289–336.

———. 1885a. On the structure and development of the skull in Mammalia. Part II. Edentata. Philosophical Transactions of the Royal Society of London, 176:1–119.

———. 1885b. On the structure and development of the skull in Mammalia. Part III. Insectivora. Philosophical Transactions of the Royal Society of London, 176:121–275.

PILZ, P.K.D., J. OSTWALD, A. KREITER, AND H.-U. SCHNITZLER. 1997. Effect of the middle ear reflex on sound transmission to the inner ear of albino rat. Hearing Research, 105:171–182.

PYE, A. 1966. The Megachiroptera and Vespertilionoidea of the Microchiroptera. Journal of Morphology, 119(2):101–119.

RAFFLES, T.S. 1821. Descriptive catalogue of a zoological collection, made on account of the honorable East Indian Company, in the island of Sumatra and its vicinity, under the direction of Sir Thomas Stamford Raffles, Lieutenant-Governor of Fort Marlborough, with additional notices illurstrative of the natural history. Transactions of the Linnean Society of London, 13:239–274.

REID, J. 1837. [Description of a new species of the genus *Perameles* (*P. lagotis*)]. Proceedings of the Zoological Society of London 1836(5):129–131.

REIG, O.A., J.A.W. KIRSCH, AND L.G. MARSHALL. 1987. Systematic relationships of the living and Neocenozoic American "opossum-like" marsupials (Suborder Didelphimorphia), with comments of the classification of these and of the Cretaceous and Paleogene New World and European metatherians. Pp. 1–89, *in* Possums and Opossums: Studies in Evolution (M. Archer, ed.). Surrey Beatty & Sons and the Royal Zoological Society of New South Wales, Chipping Norton.

REINBACH, W. 1952a. Zur Entwicklung des Primordialcraniums von *Dasypus novemcinctus* Linné (*Tatusia novemcinta* Lesson) I. Zeitschrift für Morphologie und Anthropologie, 44:375–444.

———. 1952b. Zur Entwicklung des Primordialcraniums von *Dasypus novemcinctus* Linné (*Tatusia novemcinta* Lesson) II. Zeitschrift für Morphologie und Anthropologie, 45: 1–72.

ROBINSON, A. (ED.). 1921. Cunningham's Manual of Practical Anatomy, Volume Third: Head and Neck, 7th edition. William Wood and Company, New York. 568 pp.

RODRÍGUEZ-VÁZQUEZ, J.F. 2005. Development of the stapes and associated structures in human embryos. Journal of Anatomy, 207:165–173.

RODRÍGUEZ-VÁZQUEZ, J.F., M. YAMAMOTO, S. ABE, Y. KATORI, AND G. MURAKAMI. 2018. Development of the human incus with special reference to the detachment from the chondrocranium to be transferred into the middle ear. The Anatomical Record, 301:1405–1415.

ROUGIER, G.W., AND J.R. WIBLE. 2006. Major changes in the mammalian ear region and basicranium. Pp. 269–311, *in* Amniote Paleobiology: Perspectives on the Evolution of Mammals, Birds, and Reptiles (M.T. Carrano, T.J. Gaudin, R.W. Blob, and J.R. Wible, eds.). University of Chicago Press, Chicago.

RÜPPELL, E. 1842. Säugethiere aus der Ordnung der Nager, beobachtet in nordöstlichen Afrika. Museum Senckenbergianum, 3:99–116.

SANBORN, C.C. 1951. Two new mammals from southern Peru. Fieldiana: Zoology, 32:117–124.

SÁNCHEZ-VILLAGRA, M.R., AND A.M. FORASIEPI. 2017. On the development of the chondrocranium and the histological anatomy of the head in perinatal stages of marsupial mammals. Zoological Letters, 3:1.

SÁNCHEZ-VILLAGRA, M.R., S. GEMBALLA, S. NUMMELA, K.K. SMITH, AND W. MAIER. 2002. Ontogenetic and phylogenetic transformations of the ear ossicles in marsupial mammals. Journal of Morphology, 251:219–238.

SÁNCHEZ-VILLAGRA, M.R., AND J.R. WIBLE. 2002. Patterns of evolutionary transformation in the petrosal bone and some basicranial features in marsupial mammals, with special reference to didelphids. Journal of Zoological Systematics and Evolutionary Research, 40: 26–45.

SCHLITTER, D.A. 1973. A new species of gerbil from South West Africa with remarks on *Gerbillus tytonis* Bauer and Niethammer, 1959 (Rodentia: Gerbillinae). Bulletin Southern California Academy of Sciences, 72:13–18.

SCHMELZLE, T., S. NUMELLA, AND M.R. SÁNCHEZ-VILLAGRA. 2005. Phylogenetic transformations of the ear ossicles in marsupials mammals, with special reference to diprotodontians: a character analysis. Annals of Carnegie Museum, 74(3):189–200.

SEGALL, W. 1970. Morphological parallelisms of the bulla and auditory ossicles in some insectivores and marsupials. Fieldiana: Zoology, 51:169–205.

SHARPEY, W., A. THOMSON, AND E.A. SCHÄFER (EDS.). 1878. Quain's Elements of Anatomy, Volume II, 8th edition. William Wood and Co., New York. 850 pp.

SHAW, G. 1794. Zoology of New Holland. J. Sowerby, London.

———. 1797. The Naturalist's Miscellany: or Coloured Figures of Natural Objects, Drawn and Described Immediately from Nature. Vol. 8. E. Nodder, London.

———. 1800. General Zoology. Kearsley, London.

SHUTE, C.C.D. 1956. The evolution of the mammalian eardrum and tympanic cavity. Journal of Anatomy, 90:261–281.

SISSON, S. 1914. The Anatomy of the Domestic Animals, Second Edition. W.B. Saunders Company, Philadelphia and London. 930 pp.

SPATZ, W.B. 1964. Beitrag zur Kenntnis der Ontogenese des Cranium von *Tupaia glis* (Diard 1820). Gegenbaurs Morphologsiches Jahrbuch, 106:321–416.

STIRLING, E.C. 1889. Transactions of the Royal Society of South Australia, 12:158.

———. 1891. Description of a new genus and species of Marsupialia, *Notoryctes typhlops*. Transactions of the Royal Society of South Australia, 14:154–187.

STRANDRING, S. (ED.). 2008. Gray's Anatomy. 40th edition. Churchill Livingstone. 1551 pp.

THOMAS, O. 1887. Description of a new Papuan phalanger. The Annals and Magazine of Natural History, series 5, 19:146–147.

———. 1888. Catalogue of the Marsupialia and Monotremata in the Collections of the British Museum (Natural History). British Museum (Natural History), London.

———. 1894. On *Micoureus* griseus*, Desm., with the description of a new genus and species of Didelphyidae. The Annals and Magazine of Natural History, series 6, 14:184–188.

———. 1897. On some new phalangers of the genus *Pseudocheirus*. Annali Del Museu Civico Di Storia Naturale Di Genova, 18:142–146.

TOEPLITZ, C. 1920. Bau und Entwicklung des Knorpelschädels von *Didelphis marsupialis*. Zoologica, Stuttgart, 27:1–84.

TOMES, R.F. 1863. Notice of a new American form of marsupial. Proceedings of the Zoological Society of London, 1863:50–51.

WAGNER, A. 1842. Diagnosen neuer Arten brasilischer Säugethiere. Archiv für Naturgeschichte, 8(1):356–362.

WANG, J., J.R. WIBLE, B. GUO, S.L. SHELLEY, H. HU, AND S. BI. 2021. A monotreme-like auditory apparatus in a Middle Jurassic haramiyidan. Nature, 590:279–283.

WATERHOUSE, G.R. 1836. Description of a new genus of mammiferous animals from New Holland, which will probably be found to belong to the marsupial type. Proceedings of the Zoological Society of London 1836(4):69-70.

———. 1841. The Naturalist's Library Conducted by Sir William Jardine. Mammalia Volume. XI. Marsupialia or Pouched Animals. W. H. Lizars, Edinburgh. 323 pp., +34 plates.

WIBLE, J.R. 1990. Late Cretaceous marsupial petrosal bones from North America and a cladistic analysis of the petrosal in therian mammals. Journal of Vertebrate Paleontology, 10(2):183–205.

———. 2003. On the cranial osteology of the short-tailed opossum *Monodelphis brevicaudata* (Didelphidae, Marsupialia). Annals of Carnegie Museum, 72(3):137–202.

———. 2009. The ear region of the pen-tailed treeshrew, *Ptilocercus lowii* Gray, 1848 (Placentalia, Scandentia, Ptilocercidae). Journal of Mammalian Evolution, 16(3):199–234.

———. 2010. Petrosal anatomy of the nine-banded armadillo, *Dasypus novemcinctus* Linnaeus, 1758 (Mammalia, Xenarthra, Dasypodidae). Annals of Carnegie Museum, 79(1):1–28.

WIBLE, J.R., AND J.A. HOPSON. 1993. Basicranial evidence for early mammal phylogeny. Pp. 45–62, *in* Mammal Phylogeny: Mesozoic Differentiation, Multituberculates, Monotremes, Early Therians, and Marsupials (F.S. Szalay, M.J. Novacek, and M.C. McKenna, eds.). Springer Verlag, New York.

———. 1995. Homologies of the prootic canal in mammals and non-mammalian cynodonts. Journal of Vertebrate Paleontology, 15(3):331–356.

WIBLE, J.R., AND S.L. SHELLEY. 2020. Anatomy of the petrosal and middle ear of the brown rat, *Rattus norvegicus* (Berkenhout, 1769) (Rodentia, Muridae). Annals of Carnegie Museum, 86(1):1–35.

WIBLE, J.R., AND M. SPAULDING. 2013. On the cranial osteology of the African palm civet, *Nandinia binotata* (Gray, 1830) (Mammalia, Carnivora, Feliformia). Annals of Carnegie Museum, 82(1):1–114.

WILSON, D.E., AND D.M. REEDER (EDS.). 2005. Mammals Species of the World: A Taxonomic and Geographic Reference. 3rd Edition. Johns Hopkins University Press, Baltimore.

ZELLER, U. 1983. Zur Ontogenese und Morphologie des Craniums von *Tupaia belangeri* (Tupaiidae, Scandentia, Mammalia). Medical Dissertation, University of Göttingen, Göttingen.

ZHENG, X.-T., S.-D. BI, X.-L. WANG, AND J. MENG. 2013. A new arboreal haramiyid shows the diversity of crown mammals in the Jurassic period. Nature, 500(7461):199–202.

ZIMMERMANN, E.A.W. 1780. Geographische Geschichte der Menschen, und der allgemein verbreiteten vierfüssigen Thiere. Zweiter Band. Wenganschen Buchhandlung, Leipzig.

APPENDIX 1. Marsupial specimens on DigiMorph.org with available coronal slice movies studied here.
(*continued on the following page*)

Didelphimorphia

Chironectes minimus (Zimmerman, 1780), AMNH 129701, Ms. Jeri Rodgers, 2009, "Chironectes minimus" (On-line), Digital Morphology. Accessed November 2, 2020 at http://digimorph.org/specimens/Chironectes_minimus/;

Didelphis virginiana Kerr, 1792, TMM M-2517, Dr. Ted Macrini, 2005, "Didelphis virginiana" (On-line), Digital Morphology. Accessed November 2, 2020 at http://digimorph.org/specimens/Didelphis_virginiana/;

Monodelphis domestica (Wagner, 1842), TTM M-7595, Dr. Ted Macrini, 2001, "Monodelphis domestica" (On-line), Digital Morphology. Accessed November 2, 2020 at http://digimorph.org/specimens/Monodelphis_domestica/day27/;

Monodelphis domestica (Wagner, 1842), TMM M-7536, Dr. Ted Macrini, 2001, "Monodelphis domestica" (On-line), Digital Morphology. Accessed November 2, 2020 at http://digimorph.org/specimens/Monodelphis_domestica/day48/;

Monodelphis domestica (Wagner, 1842), TMM M-8266, Dr. Ted Macrini, 2009, "Monodelphis domestica" (On-line), Digital Morphology. Accessed November 2, 2020 at http://digimorph.org/specimens/Monodelphis_domestica/day56/;

Monodelphis domestica (Wagner, 1842), TMM M-7539, Dr. Ted Macrini, 2001, "Monodelphis domestica" (On-line), Digital Morphology. Accessed November 2, 2020 at http://digimorph.org/specimens/Monodelphis_domestica/day57/;

Monodelphis domestica (Wagner, 1842), TMM M-7542, Dr. Ted Macrini, 2001, "Monodelphis domestica" (On-line), Digital Morphology. Accessed November 2, 2020 at http://digimorph.org/specimens/Monodelphis_domestica/day75/;

Monodelphis domestica (Wagner, 1842), TMM M-7545, Dr. Ted Macrini, 2001, "Monodelphis domestica" (On-line), Digital Morphology. Accessed November 2, 2020 at http://digimorph.org/specimens/Monodelphis_domestica/day90/;

Monodelphis domestica (Wagner, 1842), TMM M-7599, Dr. Ted Macrini, 2001, "Monodelphis domestica" (On-line), Digital Morphology. Accessed November 2, 2020 at http://digimorph.org/specimens/Monodelphis_domestica/adult/;

Paucituberculata

Caenolestes fuliginosus (Tomes, 1863), KU 124015, Dr. Ted Macrini, 2007, "Caenolestes fuliginosus" (On-line), Digital Morphology. Accessed November 2, 2020 at http://digimorph.org/specimens/Caenolestes_fuliginosus/;

Microbiotheria

Dromiciops gliroides Thomas, 1894, FMNH 127463, Dr. Ashley Gosselin-Ildari, 2006, "Dromiciops gliroides" (On-line), Digital Morphology. Accessed November 2, 2020 at http://digimorph.org/specimens/Dromiciops_gliroides/

Dasyuromorphia

Dasyurus hallucatus Gould, 1842, TMM M-6921, Dr. Ted Macrini, 2005, "Dasyurus hallucatus" (On-line), Digital Morphology. Accessed November 2, 2020 at http://digimorph.org/specimens/Dasyurus_hallucatus/;

Myrmecobius fasciatus Waterhouse, 1836, AMNH 155328, Dr. Ashley Gosselin-Ildari, 2007, "Myrmecobius fasciatus" (On-line), Digital Morphology. Accessed November 2, 2020 at http://digimorph.org/specimens/Myrmecobius_fasciatus/;

Sarcophilus laniarius (Owen, 1838), USNM 307639, DigiMorph Staff, 2004, "Sarcophilus laniarius" (On-line), Digital Morphology. Accessed November 2, 2020 at http://digimorph.org/specimens/Sarcophilus_laniarius/;

Sminthopsis crassicaudata (Gould, 1844), AMNH 126686, Dr. Ted Macrini, 2009, "Sminthopsis crassicaudata" (On-line), Digital Morphology. Accessed November 2, 2020 at http://digimorph.org/specimens/Sminthopsis_crassicaudata/;

Peramelemorphia

Echymipera kalubu (Fischer, 1829), AMNH 190970, Dr. Ted Macrini, 2008, "Echymipera kalubu" (On-line), Digital Morphology. Accessed November 2, 2020 at http://digimorph.org/specimens/Echymipera_kalubu/;

Isoodon macrourus (Gould, 1842), TMM M-6922, Dr. Ted Macrini, 2005, "Isoodon macrourus" (On-line), Digital Morphology. Accessed November 2, 2020 at http://digimorph.org/specimens/Isoodon_macrourus/;

Macrotis lagotis (Reid, 1837), AMNH 74486, Dr. Ashley Gosselin-Ildari, 2007, "Macrotis lagotis" (On-line), Digital Morphology. Accessed November 2, 2020 at http://digimorph.org/specimens/Macrotis_lagotis/;

Notoryctemorphia

Notoryctes typhlops (Stirling, 1889), AMNH 202107, Ms. Jeri Rodgers, 2008, "Notoryctes typhlops" (On-line), Digital Morphology. Accessed November 2, 2020 at http://digimorph.org/specimens/Notoryctes_typhlops/;

Diprotodontia

Acrobates pygmaeus (Shaw, 1794), AMNH 155057, DigiMorph Staff, 2016, "Acrobates pygmaeus" (On-line), Digital Morphology. Accessed April 6, 2021 at http://digimorph.org/specimens/Acrobates_pygmaeus/;

Cercartetus caudatus (Milne-Edwards, 1877), AMNH 155090, Dr. Ted Macrini, 2008, "Cercartetus caudatus" (On-line), Digital Morphology. Accessed November 2, 2020 at http://digimorph.org/specimens/Cercartetus_caudatus/;

Dactylopsila trivirgata Gray, 1858, AMNH 104040, Ms. Jeri Rodgers, 2009, "Dactylopsila trivirgata" (On-line), Digital Morphology. Accessed November 2, 2020 at http://digimorph.org/specimens/Dactylopsila_trivirgata/;

Dendrolagus lumholtzi Collett, 1884, AMNH 65254, Dr. Ted Macrini, 2007, "Dendolagus lumholtzi" (On-line), Digital Morphology. Accessed November 2, 2020 at http://digimorph.org/specimens/Dendrolagus_lumholtzi/;

Hemibelideus lemuroides Collett, 1884, AMNH 154375, Ms. Jeri Rodgers, 2009, "Dactylopsila trivirgata" (On-line), Digital Morphology. Accessed November 2, 2020 at http://digimorph.org/specimens/Hemibelideus_lemuroides/;

Lasiorhinus sp., NMV C33128, Dr. Alana Sharp, 2016, "Lasiorhinus sp." (On-line), Digital Morphology. Accessed November 2, 2020 at http://digimorph.org/specimens/Lasiorhinus_sp/;

Macropus rufus (Desmarest, 1822), NVM C23045, Dr. Alana Sharp, 2015, "Macropus rufus" (On-line), Digital Morphology. Accessed November 2, 2020 at http://digimorph.org/specimens/Macropus_rufus/skull/;

APPENDIX 1. Marsupial specimens on DigiMorph.org with available coronal slice movies studied here.
(*continued from the previous page*)

Petauroides volans Thomas, 1888, AMNH 15005, Ms. Jeri Rodgers, 2009, "Petauroides volans" (On-line), Digital Morphology. Accessed November 2, 2020 at http://digimorph.org/specimens/Petauroides_volans/;
Petropseudes dahli (Collett, 1895), AMNH 183391, Ms. Jeri Rodgers, 2009, "Petropseudes dahli" (On-line), Digital Morphology. Accessed November 2, 2020 at http://digimorph.org/specimens/Petropseudes_dahli/;
Phalanger orientalis Pallas, 1766, AMNH 157211, Dr. Ted Macrini, 2010, "Phalanger orientalis" (On-line), Digital Morphology. Accessed November 2, 2020 at http://digimorph.org/specimens/Phalanger_orientalis/;
Phascolarctos cinereus (Goldfuss, 1817), TMM M-2946, DigiMorph Staff, 2004, "Phascolarctos cinereus" (On-line), Digital Morphology. Accessed November 2, 2020 at http://digimorph.org/specimens/Phascolarctos_cinereus/;
Potorous tridactylus Desmarest, 1804, AMNH 65337, Dr. Ted Macrini, 2009, "Potorous tridactylus" (On-line), Digital Morphology. Accessed November 2, 2020 at http://digimorph.org/specimens/Potorous_tridactylus/;
Pseudocheirus occidentalis (Thomas, 1888), TMM M-847, Dr. Ted Macrini, 2007, "Pseudocheirus occidentalis" (On-line), Digital Morphology. Accessed November 2, 2020 at http://digimorph.org/specimens/Pseudocheirus_occidentalis/;
Pseudochirops cupreus (Thomas, 1897), AMNH 151829, Ms. Jeri Rodgers, 2009, "Pseudochirops cupreus" (On-line), Digital Morphology. Accessed November 2, 2020 at http://digimorph.org/specimens/Pseudochirops_cupreus/;
Pseudochirulus forbesi (Thomas, 1887), AMNH 104136, Ms. Jeri Rodgers, 2009, "Pseudochirulus forbesi" (On-line), Digital Morphology. Accessed November 2, 2020 at http://digimorph.org/specimens/Pseudochirulus_forbesi/;
Trichosurus vulpecula (Kerr, 1792), TMM M-849, Dr. Ted Macrini, 2007, "Trichosurus vulpecula" (On-line), Digital Morphology. Accessed November 2, 2020 at http://digimorph.org/specimens/Trichosurus_vulpecula/;
Vombatus ursinus (Shaw, 1800), TMM M-2953, DigiMorph Staff, 2004, "Vombatus ursinus" (On-line), Digital Morphology. Accessed November 2, 2020 at http://digimorph.org/specimens/Vombatus_ursinus/
Wallabia bicolor Desmarest, 1804, TMM M-4169, Dr. Ted Macrini, 2005, "Wallabia bicolor" (On-line), Digital Morphology. Accessed November 2, 2020 at http://digimorph.org/specimens/Wallabia_bicolor/.

APPENDIX 2. Marsupial specimens downloaded and studied from MorphoSource.org.

Didelphimorphia
Caluromys sp., DU EA 161, head and partial neck, https://www.morphosource.org/concern/biological_specimens/0000S5302?locale=en;
Caluromysiops irrupta Sanborn, 1951, FMNH 60698, skeleton, https://www.morphosource.org/concern/biological_specimens/000S24214?locale=en;
Didelphis marsupialis Linnaeus, 1758, DU BAA 0164, skull and postcranial skeleton, https://www.morphosource.org/concern/biological_specimens/0000S5277?locale=en;
Didelphis sp., DU EA 202, whole body wet specimen, https://www.morphosource.org/concern/biological_specimens/0000S6489?locale=en;
Monodelphis domestica (Wagner, 1842), AMNH 261241, cranium, https://www.morphosource.org/concern/biological_specimens/0000S5433?locale=en;

Paucituberculata
Rhyncholestes raphanurus Osgood, 1924, FMNH 127476, whole body wet specimen, https://www.morphosource.org/concern/biological_specimens/000S24219?locale=en;

Microbiotheria
Dromiciops gliroides Thomas, 1894 (=*Dromciops australis*), UMMZ 156354, skeleton, https://www.morphosource.org/concern/biological_specimens/000S19901?locale=en;

Peramelemorphia
Isoodon obesulus (Shaw, 1797) (=*Perameles obesula*), UMZC A7. 4/5, skeleton, https://www.morphosource.org/concern/biological_specimens/000S24233?locale=en;

Notoryctemorphia
Notoryctes typhlops (Stirling, 1889), UMZC A5. 1/1, skeleton, https://www.morphosource.org/concern/biological_specimens/000S19907?locale=en.